AD-A054 706 GRUMMAN AEROSPACE CORP BETHPAGE N Y RESEARCH DEPT F/G 19/1
ANALYSIS OF THE OPTICAL MEMORY AND TRANSDUCER REQUIREMENTS FOR --ETC(U)
FEB 78 K G LEIB, M R WOHLERS

UNCLASSIFIED RE-554 NL

| OF |
AD
A054706

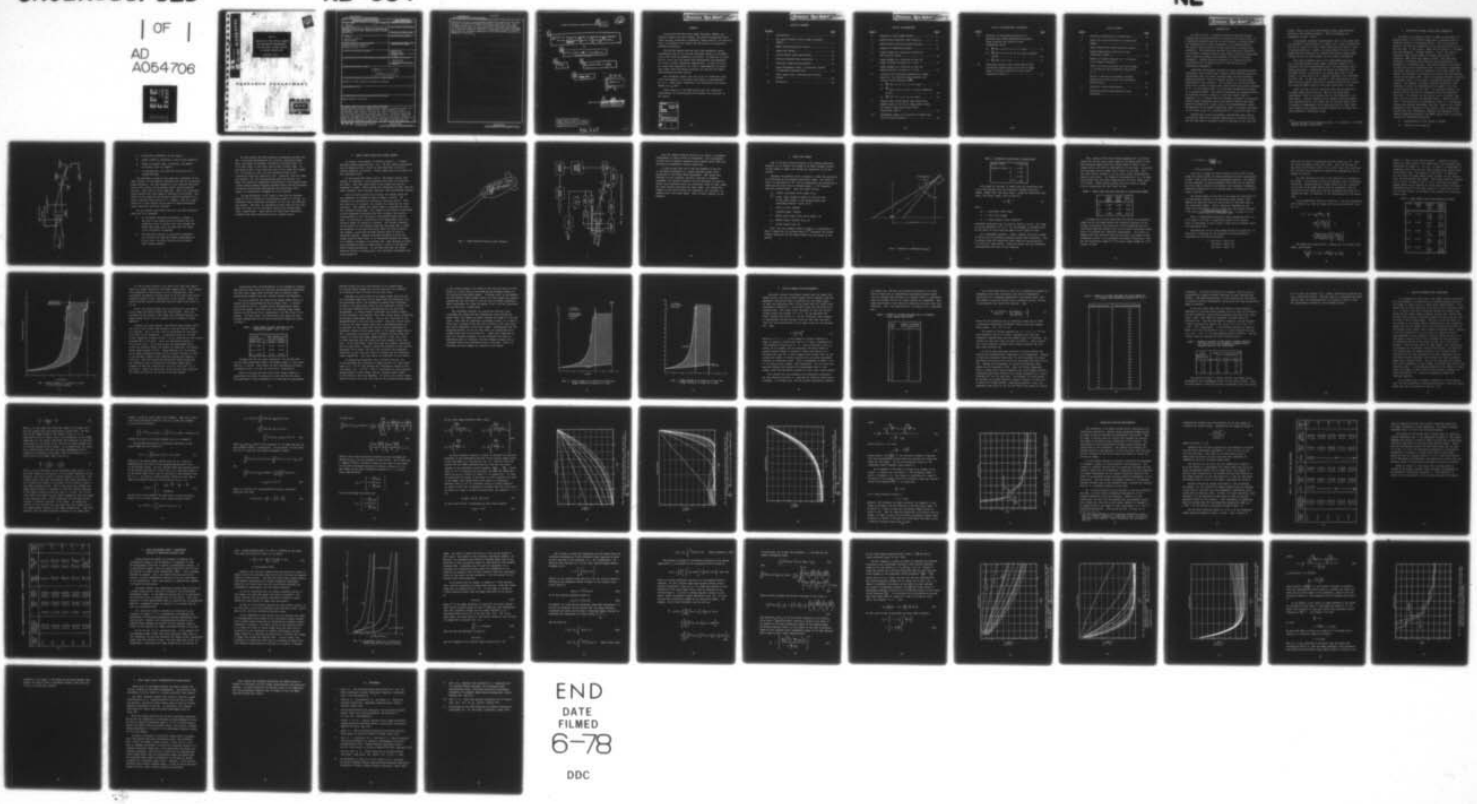

END
DATE
FILMED
6-78
DDC

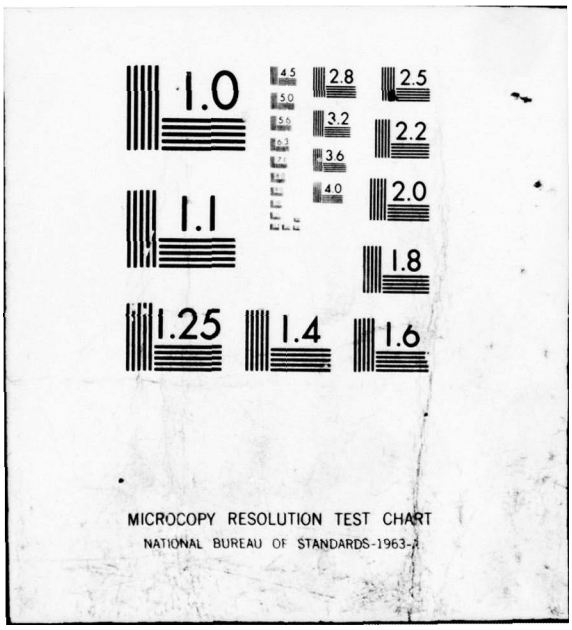
1.0
1.1
1.25
1.4
1.6
1.8
2.0
2.2
2.5
2.8
3.2
3.6
4.0
4.5
5.0
5.6
MICROCOPY RESOLUTION TEST CHART
NATIONAL BUREAU OF STANDARDS-1963-A

RE-554

ANALYSIS OF THE OPTICAL MEMORY AND TRANSDUCER REQUIREMENTS FOR THE OMFIC SYSTEM APPLIED TO GUIDED PROJECTILES

February 1978

UNCLASSIFIED

SECURITY CLASSIFICATION OF THIS PAGE *(When Data Entered)*

REPORT DOCUMENTATION PAGE		READ INSTRUCTIONS BEFORE COMPLETING FORM
1. REPORT NUMBER RE-554	2. GOVT ACCESSION NO.	3. RECIPIENT'S CATALOG NUMBER
4. TITLE *(and Subtitle)* ANALYSIS OF THE OPTICAL MEMORY AND TRANSDUCER REQUIREMENTS FOR THE OMFIC SYSTEM APPLIED TO GUIDED PROJECTILES		5. TYPE OF REPORT & PERIOD COVERED 6. PERFORMING ORG. REPORT NUMBER
7. AUTHOR(s) Kenneth G. Leib and Ronald Wohlers		8. CONTRACT OR GRANT NUMBER(s)
9. PERFORMING ORGANIZATION NAME AND ADDRESS Grumman Aerospace Corporation Bethpage, New York 11714		10. PROGRAM ELEMENT, PROJECT, TASK AREA & WORK UNIT NUMBERS
11. CONTROLLING OFFICE NAME AND ADDRESS		12. REPORT DATE February 1978 13. NUMBER OF PAGES 68
14. MONITORING AGENCY NAME & ADDRESS *(if different from Controlling Office)*		15. SECURITY CLASS. *(of this report)* UNCLASSIFIED 15a. DECLASSIFICATION/DOWNGRADING SCHEDULE

16. DISTRIBUTION STATEMENT *(of this Report)*

DISTRIBUTION STATEMENT A
Approved for public release;
Distribution Unlimited

17. DISTRIBUTION STATEMENT *(of the abstract entered in Block 20, if different from Report)*

Approved for public release, distribution unlimited

18. SUPPLEMENTARY NOTES

19. KEY WORDS *(Continue on reverse side if necessary and identify by block number)*

Missile guidance, correlator

20. ABSTRACT *(Continue on reverse side if necessary and identify by block number)*

The Optical Matched Filter Image Correlator (OMFIC) can identify targets and their number, and provide information about their bearing, positional coordinates, range interval, and velocity. Thus, it provides a new concept for the missile or projectile guidance application. The optical memory size and real time transducer update requirements are two of the most important aspects of the OMFIC system when used for guiding a projectile. An analysis of these factors shows that the memory bank requirements are manageable and within current technology capabilities. In order to cover the range from

DD FORM 1 JAN 73 1473 EDITION OF 1 NOV 65 IS OBSOLETE
S/N 0102-014-6601

UNCLASSIFIED

SECURITY CLASSIFICATION OF THIS PAGE *(When Data Entered)*

M sub f

acquisition (1.5 km) to approximately 50 meters from impact only 397 memory positions are required for highly discriminating matched filters. The transducer update rate can be set at television frame rates for guidance to 50 meters from impact at approximately $M_f = 0.5$. Under these conditions, the correlation peak should remain at $\hat{c} \geq -3$dB. Other aspects of the OMFIC memory bank and transducer requirements for missile/projectile guidance are developed in the report.

(12)

Grumman Research Department Report (14) RE-554

(6)

ANALYSIS OF THE OPTICAL MEMORY AND TRANSDUCER REQUIREMENTS FOR THE OMFIC SYSTEM APPLIED TO GUIDED PROJECTILES.

by

(10) Kenneth G. Leib and M. Ronald Wohlers
System Sciences

(12) 73 pp

(9) Research Repts

(11) February 1978

Approved by: Richard A. Scheuing
Director of Research

RE: Classified references-
Grumman Aerospace Rept. No. RE-554
Document should remain for unlimited distribution per Mr. Ronald Wohlers, Grumman Aerospace Corp.

406 165

ABSTRACT

The Optical Matched Filter Image Correlator (OMFIC) can identify targets and their number, and provide information about their bearing, positional coordinates, range interval, and velocity. Thus, it provides a new concept for the missile or projectile guidance application.

The optical memory size and real time transducer update requirements are two of the most important aspects of the OMFIC system when used for guiding a projectile. An analysis of these factors shows that the memory bank requirements are manageable and within current technology capabilities. In order to cover the range from acquisition (1.5 km) to approximately 50 meters from impact only 397 memory positions are required for highly discriminating matched filters.

The transducer update rate can be set at television frame rates for guidance to 50 meters from impact at approximately $M_f = 0.5$. Under these conditions, the correlation peak should remain at $\hat{c} \geq -3$dB.

Other aspects of the OMFIC memory bank and transducer requirements for missile/projectile guidance are developed in the report.

TABLE OF CONTENTS

LIST OF ILLUSTRATIONS

LIST OF ILLUSTRATIONS (CONTINUED)

LIST OF TABLES

1. INTRODUCTION

As early as 1971, a semiactive guided projectile was gun launched and functioned properly according to one report (Ref. 1). A semiactive guided projectile is one in which a selected target is illuminated with a laser designator by a forward observer. The optical return picked up by the projectile is focused upon a detector. This system was mounted in an eight-inch projectile and utilized a quadrant detector from which a position proportional error signal for guidance was derived; the field of view was 36 degrees. Further work was conducted on a five-inch guided projectile with a 25 degree field of view and which used proportional navigation.

Additional developments improved the laser designated guided projectiles, and in some cases, special electro-optical projectile developments were also made; although these are not considered guided projectiles, they do represent efforts to provide target identification for artillery. One of these is a 155 mm artillery shell with a charge coupled device (CCD) television system contained in it. At last report (Ref. 2) it had been successfully operated in a simulated flight. This effort represents the growing interest of artillery forces to develop a "fire and forget" type of scenario, i.e., a system that will continue to guide the projectile without human assistance such as the forward observer who designated the target with a laser beam in the aforementioned system. The maturity of the guided projectiles effort is further reflected in the recent issue of a specification for a projectile (Ref. 3).

Several more recent developments demonstrated that optical correlators might have potential application in artillery shells (or for that matter, missiles) where in addition to the "fire and

forget" feature one could add automated target identification, selection, and terminal guidance. These developments are documented in Refs. 4 and 5.

A subsequent correlator investigation (Ref. 6) has shown that the parametric sensitivities of a target (e.g., scale, orientation) are not so severe as to make target identification within a class of targets difficult. Rather, a limited number of views of one target would be sufficient to identify the desired target among similar but not the same targets (at any target orientation).

This report examines some of the requirements necessary for an optical matched filter image correlator (OMFIC[†]) to be considered for both identification and a fire and forget type of guided projectile. Considering the amount of information that the OMFIC system, in principle, can reveal about one or more targets, it would seem to be a logical candidate to be considered for this role. In the next section, a brief description of the OMFIC system is given after which a general review of the concept for using the OMFIC system in this type application is given.

There are many critical questions which the application of an OMFIC system raises such as: What is the memory bank requirement? What is the update rate for the transducer? and many others. Specific answers are not always possible without a full specification for the system but the sections which follow do present an examination of the questions and, at least, give some bounds on the problem from which answers may be drawn for a more definitive, prescribed system.

[†] Optical Matched Filter Image Correlator, U.S. Patent No. 3,779,492, Grumman Aerospace Corporation

2. THE OPTICAL MATCHED FILTER IMAGE CORRELATOR

The OMFIC is a system in which an image is presented to a matched filter of the desired target and a comparison made to determine whether a correlation exists. This is the process common to all optical correlators of the type described by van der Lugt (Ref. 7) and others. There are two aspects to the OMFIC that are different: Consider Figure 1. First, the image is presented (with natural light or through some assist) to a transducer (XDR) where the image is stored. The image then modulates a collimated laser beam and the modulated beam is presented to a transform lens. The second feature of the OMFIC is that the Fourier transforming lens is a multiple holographic lens which takes the Fourier transform of the input image, and directs the transform in replication to each of the many matched filters in the memory bank. Each of the matched filters represents a different aspect of one target, or different aspects of many targets. For example, the memory bank may contain all views necessary to cover all orientations of a target of one size, or all orientations of many sizes. For practical reasons, the matched filters are made in conjunction with the holographic lens used. For example, if the lens is a 10 x 10 array, then there would be at least 100 matched filters. (There could be more -- this questions is investigated in Ref. 6.) The matched filters are prepared beforehand, and thus, there is an a priori knowledge of the character of each filter. This is important because with this information, together with knowledge of the Fourier transform properties, the OMFIC system does in principle contain the following information:

- Identification of the target or targets
- Bearing of the target(s)

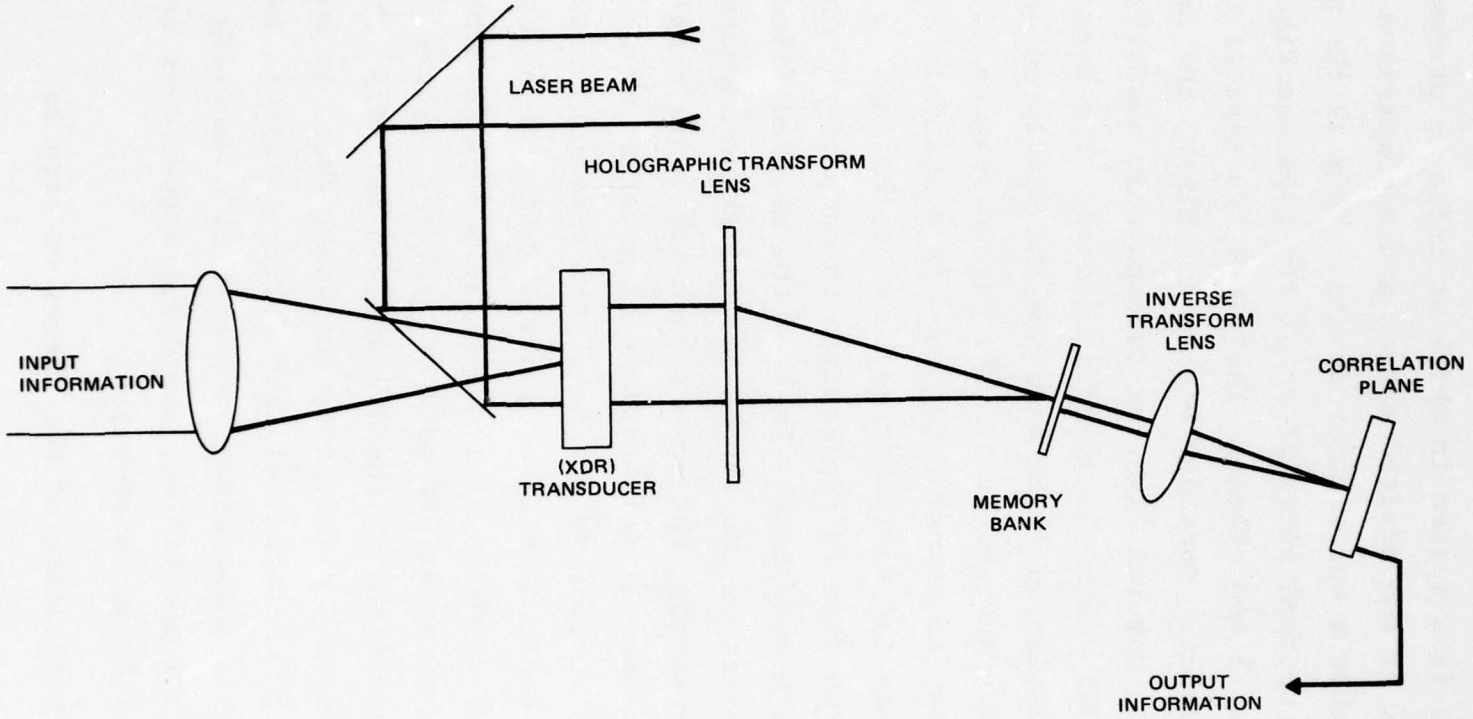

Fig. 1 Elements of Basic OMFIC System

- Positional coordinates of each target
- Range (within an interval) to each of the target(s)
- Number of targets (and, if desired, the numbers of several types of targets)
- If provided for, the speed and direction of the targets' headings

The remaining, though no less important components of the OMFIC system, are the inverse transform lens and the correlation plane processor. The lens presents to the processor the transform of the product of the matched filter optical transfer function (OTF) and the input image OTF. Thus, the correlation plane contains the input image as modified by the filter. The effect of the transform and inverse transform operations is to cause a spatial plane rotation of π radians. This is a small point but it does caution one to keep the image/correlation plane directions correctly oriented.

For the present application there are two main questions which are to be examined:

- As the guided projectile approaches a target, a new view of the target must be recorded upon the transducer every so often, and a test through the memory bank made; thus, how fast must the image on the transducer be updated?
- The particular missile or projectile considered will dictate the range and target requirements to be met; thus, how many filters must the memory bank storage contain?

We will assume (for this analysis) information derived from Ref. 6 as being representative of a typical, desirable target. Thus, the target of interest selected is an M-60 A1 tank. It is 22 feet long, 12 feet wide, and 10 feet 9 inches high. It was shown in Ref. 6 that when the scale of the image was changed by ± 20 percent in area, the autocorrelation peak in the correlation plane was reduced by 3 dB. Similarly, when the image was rotated ± 8^{o}, the autocorrelation peak was reduced 3 dB. These are called the parametric sensitivities of the target using a high optical spatial frequency matched filter and they determine the memory bank storage requirements when particular scale ranges, or orientation coverages are to be achieved.

For the projectile, a 20^{o} field of view with an incident angle of 70^{o} is assumed at an acquisition range of 1.525 km. At different times, projectile velocities of 214, 305, and 400 m/sec are assumed. The first is considered a lower limit for any case while the other two are considered nominal and extreme upper limit, respectively. These values are based upon information obtained from those experienced in the ordnance field.

3. OMFIC GUIDED PROJECTILE SYSTEM CONCEPT

In concept, the scenario is shown in Figure 2. A cannon launched guided projectile (GP - e.g., 155 mm) reaches acquisition time at apogee and has a field of view which may, or may not include target(s) of interest. These targets may fall anywhere in the observable field.

At the acquisition range turn-on, the master control unit (Figure 3) initiates a clock generator from which all functions are timed. This unit turns power on and causes the various sequences to start. These include the transducer cycling, detector array scanning, laser cycling, detection, and thresholding controls.

With all units powered and cycling, the shutter opens and the transducer is powered so that an image is stored. The transducer is postulated as cycling at twice per second. After the read cycle is complete, the shutter is closed and the laser activated. This enables the stored image to spatially modulate the collimated laser beam. This image is then Fourier transformed by the holographic transform lens which presents the spectrum simultaneously to all positions of the matched filter memory bank. At the latter, correlation of the image takes place if a tactical target of interest is present. The inverse transform of the product of the matched filter OTF and image OTF is taken and presented to the detection array which has been activated and scanned. Activation includes battery power as well as threshold setting. Signals exceeding threshold activate the target decision logic where it is determined whether the target is a primary, secondary, or tertiary one. This decision is based upon information which has been stored a priori in the matched filter during fabrication. At the same time that the target decision process is taking place, the positional coordinates are being generated.

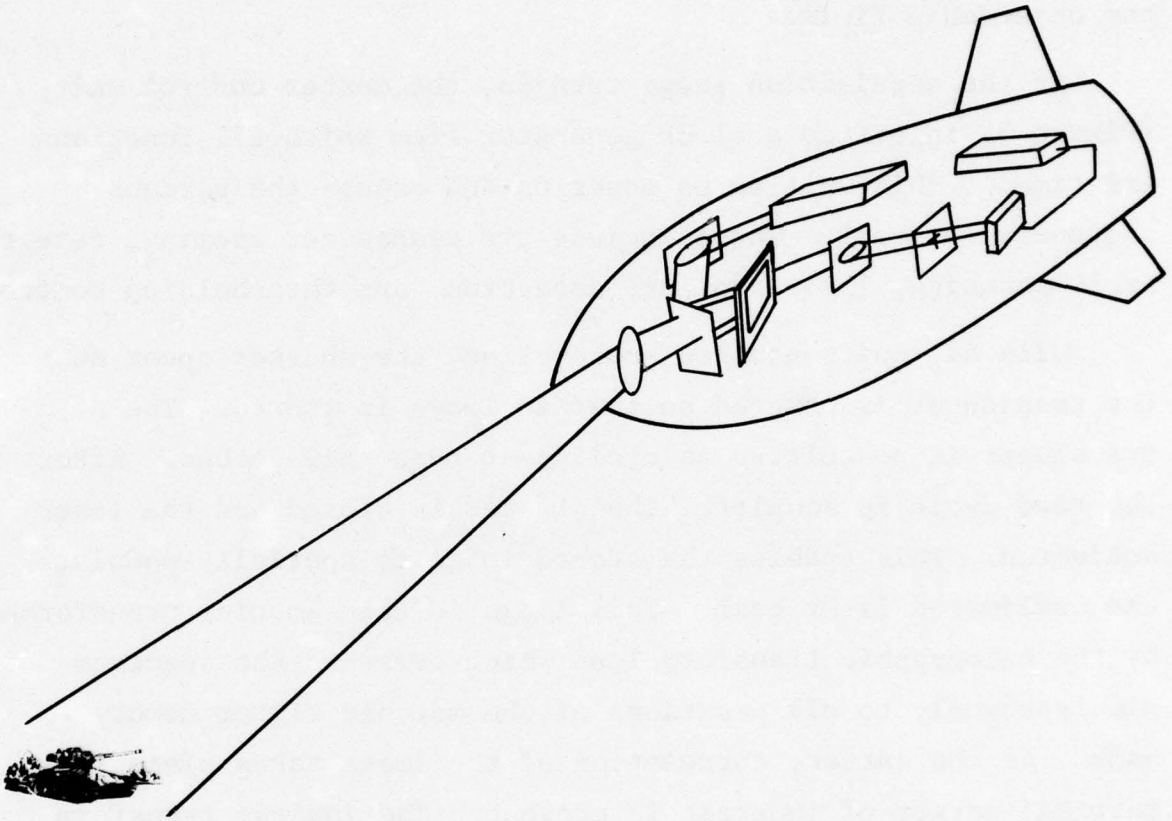

Fig. 2 OMFIC-Guided Projectile (GP) Scenario

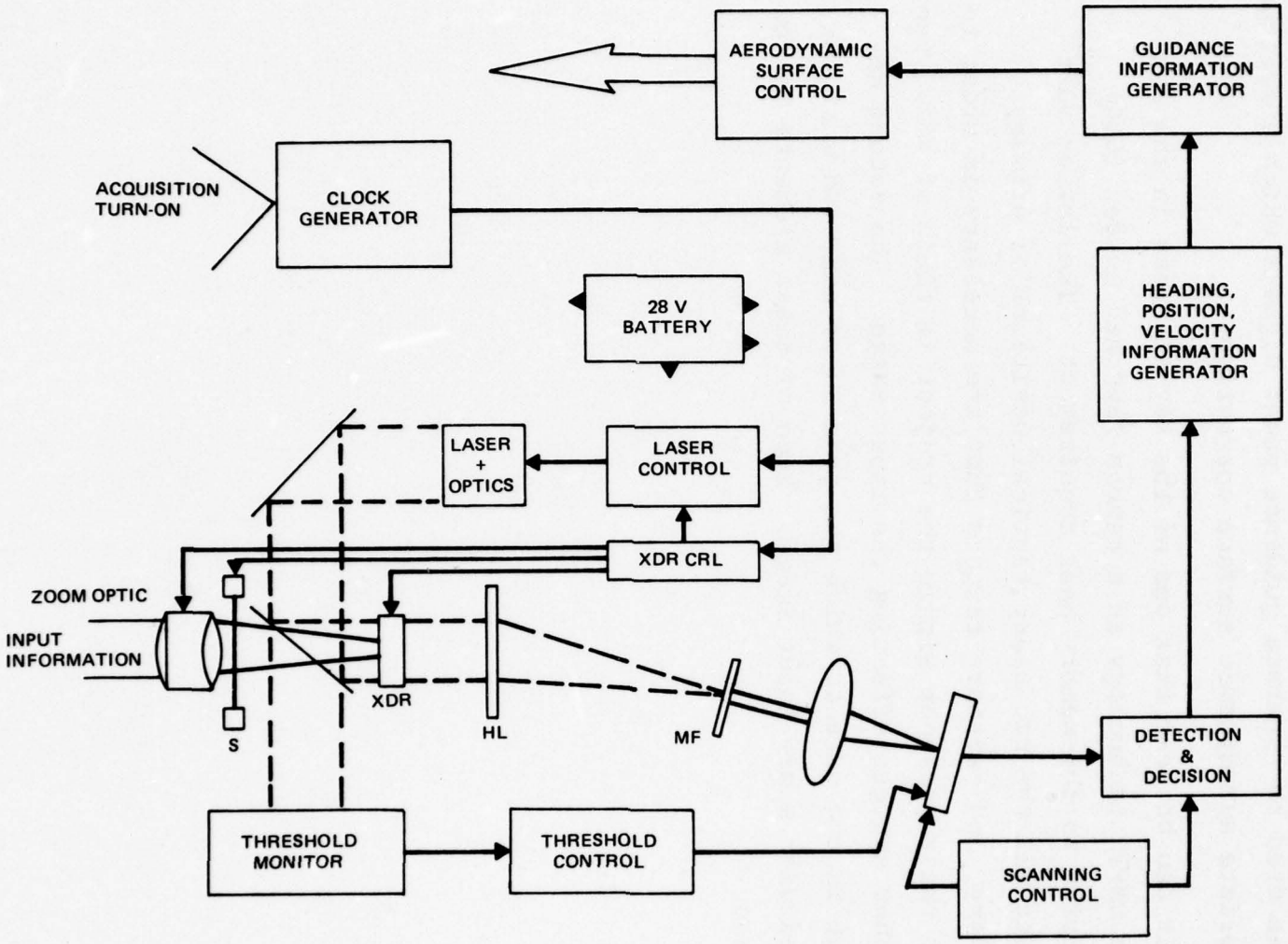

Fig. 3 OMFIC-Guided Projectile System Concept

Upon the target position decision, the offset, or guidance requirement to reduce offset is determined. This information is then used to generate guidance power signals which effect an appropriate aerodynamic surface correction.

It can be seen that one of the key elements in the use of the OMFIC technology in a cannon launched guided (CLG) projectile is the memory bank requirement. The latter must consider all the necessary tactical positions of primary, secondary, and tertiary targets that are necessary in order to detect their presence within the projectile field of view, range, and other aspects affecting the input image. The second key element is the rate at which the transducer can, and must, be updated with a new input image. Each of these elements is now examined.

4. IMAGE SIZE CHANGE

One of the most critical aspects of the guided projectile scenario, as it affects the design of an OMFIC guidance system, is the change of image size during the trajectory of the projectile.

Consider the geometry shown in Figure 4, where the projectile is illustrated at the maximum acquisition range. The field of view α is prescribed at 20^{o}, and at acquisition, the projectile is observing the scene from an incident angle $\theta = 70^{o}$ measured from the surface normal. From the figure we have

R_o optical centerline slant range in km

$R^{+,-}$ outer, inner ranges at edges of field of view in the plane normal to the ground surface and containing missile's path, in km

α field of view, degrees

θ incident angle, degrees

F OMFIC system input optic focal length, mm

L_o imaged target (linear) size, mm

S actual target size, mm

Also, from the geometry shown in Figure 4, information in Table 1 might also be obtained where $X^{L,R}$ represent the perpendicular distances off the normal plane from the target on the ground.

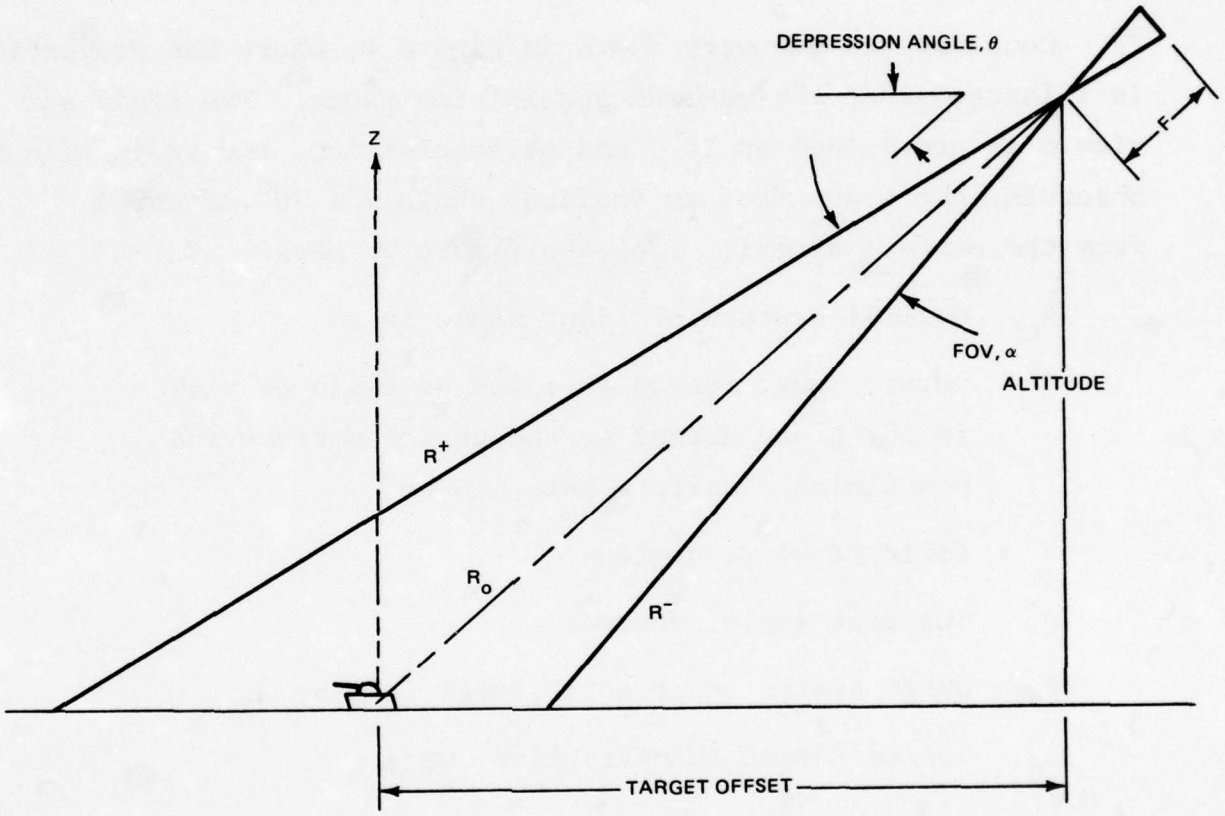

Fig. 4 Geometry of OMFIC/GP Scenario

TABLE 1 GEOMETRICAL QUANTITIES AT ACQUISITION

Target Offset		= 1.433 km
Target Altitude	H	= 0.265
	X^+	= 1.525
	X^-	= 0.530
	$X^{L,R}$	= 1.549

The target of interest is imaged upon the transducer with a size that depends upon the projectile imaging lens focal length, target size, and slant range. Along the centerline slant range, the linear target size is given by

$$L_o = \frac{F}{R_o} S \qquad (1)$$

where

R_o = centerline slant range

F = lens focal length

S = actual target linear dimension

Consistent dimensions must be used to obtain L_o in mm. The range R_o can be replaced by R^+ or R^- for the minimum, or maximum sizes in the field of view along the edges of this field of view.

As a reasonable approach, a good, commonly used focal length of 305 mm will be generally employed except where indicated. Also, a nominal value for centerline slant range for one projectile is 1.525 km at acquisition. These two values will be considered representative and used in this analysis.

Thus, using a 305 mm focal length imaging lens, the linear image size for the given slant range and 20 degree field of view and depression angle yields the values shown in Table 2 for a target such as the M-60 A1 tank which is 22 feet long. Correction has been made for the height (10.75 feet) of the tank. Also, the scale factor referred to in the usual aerial reconnaissance sense is also given. The change of approximately 3 to 1 in image size between the near slant range and the far slant range ought to be noted. These values actually form the limits in image size at acquisition for this field of view.

TABLE 2 IMAGE SIZES AND SCALE FACTORS AT ACQUISITION RANGES

	Slant Range (km)	Image Size (mm)	Scale Factor
R^-	1.043	1.962	3420
R_o	1.525	1.342	5000
R^+	2.985	0.686	9787

We might note at this point that the initial or acquisition range size of the image impacts the required resolution of the system; particularly the resolution of the transducer and the resolvable detection element size in the output correlation plane. First, we consider the transducer requirements. If we were to require that the tank have five cycles across its height (levels determined in Ref. 9 for acceptable correlative detection), then for the acquisition range of 1.5 km and a target height of 3.279 meters, we have

$$\nu = 5 \text{ cycles} \times \frac{1}{\frac{3.279M}{1500M}} \text{ rad}$$

$$\equiv 2.29 \text{ cycles/mrad}$$

If we are to image the entire field of view of 20^{o} (or 349 mrad) this would require a system resolution of (2.29 cycles/mrad) x (349) = 800 cycles across the processing aperture. For example, in the transducer we must accommodate 800 cycles in the aperture and if we take a varied 35 mm aperture this requires a transducer resolution capability of 23 cycles/mm which is within the current state of the art.

The second impact of the size of the image at acquisition is the requirement imposed on the detection plane; namely, that ideally the detector must not only respond to the peak value of the correlation signal. From a practical standpoint we can relax this requirement, in fact, based upon the results from Ref. 9 the ratio $\frac{\text{correlation spot size}}{\text{object size in correlation plane}}$ is equal to 0.34.

Thus, a corresponding detection plane requirement calls for 0.34 x 800 = 270 lines, a reasonable system in the current state of technology in which about 5 lines can be obtained across the correlation spot.

Returning now to the scale change during the trajectory, we note that in carrying out our analysis we will generally be concerned with the three velocities

$$v = 214 \text{ m/sec} \equiv \text{Mach } 0.64$$
$$305 \text{ m/sec} \equiv \text{Mach } 0.91$$
$$400 \text{ m/sec} \equiv \text{Mach } 1.19$$

which will be used in conjunction with the ranges R_o, $R^{+,-}$ which are often presented as the ratio (v/R). Thus, one or more of the values of the ratio (v/R) = 0.14, 0.20, 0.26, 0.32, and 0.38, will be used in the analysis to bracket the combinations in the ranges of interest.

For this analysis the path of the projectile is straight to the target. No allowance is made for ballistic path, or guidance correction. During projectile flight there will be a variation in the size of the image placed upon the transducer, and the variation of this image size, and the frequency with which it is changed and held, is paramount to the determination of the memory bank.

If the projectile velocity is given by v, and the acquisition slant range by R_o, then the image size will vary such that, from Eq. (1)

$$(L_i - L_o) = \frac{FS}{(R_o - vt)} - \frac{FS}{R_o}$$

$$= \frac{FS}{R_o}\left[\frac{(v/R_o)t}{1 - \left(\frac{v}{R_o}\right)t}\right] \quad \text{or} \qquad (2)$$

$$= \left[\begin{matrix}\text{Image Size at} \\ \text{Acquisition} \\ \text{on Transducer}\end{matrix}\right]\left[\frac{(v/R_o)t}{1 - \left(\frac{v}{R_o}\right)t}\right]$$

The image size change factor, allowing for the initial input image, then becomes

$$\frac{L_i - L_o}{\left(\frac{FS}{R_o}\right)} = X = \left[1 + \frac{Vt}{1 - Vt}\right] = \frac{1}{(1 - Vt)} \qquad (3)$$

where $V = (v/R_o)$ is the velocity factor. Equation (3) would enable the time history of the image size to be determined from acquisition to impact ($1 - Vt = 0$). In Table 3 a computation is summarized which shows how the image change factor varies close to the impact time. The latter is also given. In addition, for each case the image change factor is given for the running time, 50 milliseconds from impact. This table should be compared to the curves in Figure 5 for V = 0.14, 0.20 where the image change factor can be examined in closer detail near acquisition. Equivalent curves for the other values of V would fall to the left of those shown, and asymptotically approach the respective impact times.

TABLE 3 IMAGE CHANGE FACTOR NEAR PROJECTILE IMPACT

v/R	Impact Time	Running Time (sec)	Image Change Factor X
0.14	7.143	6.90	29.4
		7.00	50.0
		7.093	143.3
0.20	5.000	4.85	33.3
		4.9	50.0
		4.95	100.0
0.26	3.846	3.6	15.63
		3.7	26.32
		3.796	76.69
0.32	3.125	3.05	41.7
		0.075	62.5
		3.1	125.0
0.38	2.632	2.5	20.0
		2.582	53.08
		2.6	83.33

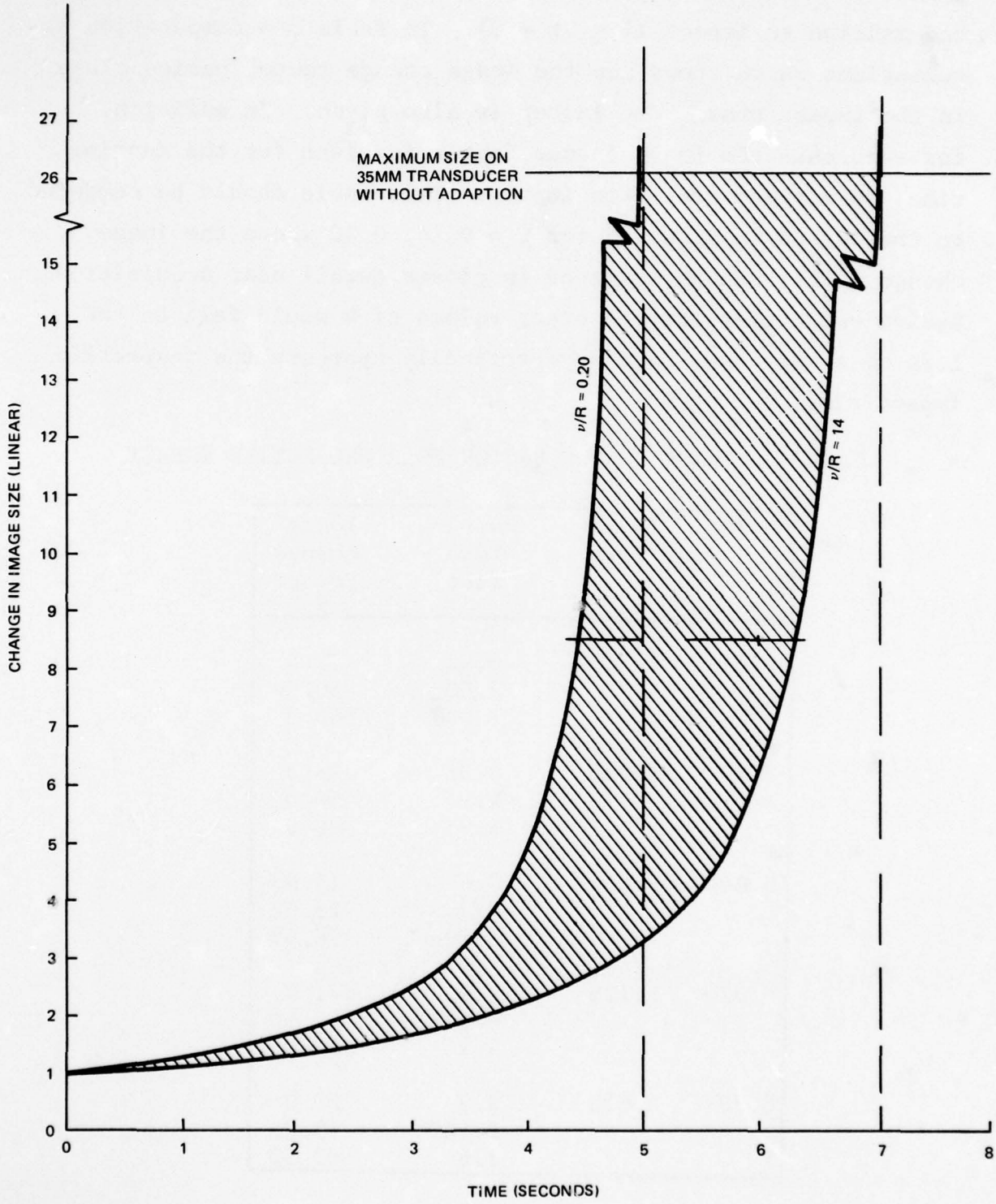

Fig. 5 Image Changes as a Function of Time for Two Velocity Ratios

It can be seen in Table 3 (or from $X'(t)$) that near impact there is a large increase in the image change factor. The question to be answered is, what value of X is a limiting one? This illustrates an example in which there is no one value that can be specified without a full prescription of the system. Rather we would postulate several conditions and then enable some bound to be set.

First, the initial image size at acquisition is determined by the range and optical input lens focal length. Then, the allowance of the growth of the image size expressed through the image change factor, will be limited by the transducer format employed.

Consider the focal length. The maximum image change factor will occur, for a fixed time interval, when the initial image is a minimum. This, in turn, will be established by the resolution limit of the transducer. A reasonable value for the MTF of the transducer is given in Ref. 4 as 20 cycles/mm for the usually accepted MTF = 0.25 point. Thus, the resolution element is 0.05 mm per cycle. If we also accept the requirement that 5 cycles are required across the target for detection, the minimum target width becomes 0.25 mm. Using Equation (1), the minimum focal length allowable becomes 204 mm (using R^+ because it leads to the smallest image at the centerline acquisition range R_o = 1.525 km). With the resolution-determined minimum image size, the transducer will be filled when the image change factor becomes 144 and 228, respectively, for 36 x 24 mm and 57 x 57 mm formats. These two sizes were chosen because they represent the usable portions of the 35 and 70 mm film formats.

Discussions with one investigator in the transducer research area indicate that these two sizes are technologically acceptable and that sizes larger than 70 mm may lead to electric field distribution problems and thus, require further investigation.

We could establish the limit on the image change factor in another way by prescribing the focal length first. A typical value would be 305 mm, a common aerial reconnaissance camera, lens focal length. With this lens, the limiting image change factors are 26.08 and 42.47, respectively, for the 35 and 70 mm formats. In these cases, the centerline slant range was used. Several computations for the three acquisition ranges are given in Table 4.

TABLE 4 IMAGE CHANGE FACTORS REQUIRED TO FILL TRANSDUCER FORMATS (FL = 305 mm)

Initial Acquisition Range (km)	Image Change Factor to Fill Format	
	35 mm	70 mm
$R^+ = 2.985$	51.02	83.09
$R_o = 1.525$	26.08	42.47
$R^- = 1.043$	17.84	29.05

Consider now the two lower velocities, 214 and 305 m/sec for the same acquisition range, the minimum range, or near field, when $R_o = 1.525$ km. The results of this calculation are shown in Figures 6 and 7 for the two velocities, respectively.

Here we see that the near field scene image change is a significant one while the opposite is true for the far scene. The importance of this difference is in deriving the appropriate

matched filters for the scale interval to be covered since the initial small changes for the far scene are not identical in an absolute sense to those for the near scene.

Although the upper bound on the image change factor is set by the maximum image that can be placed upon the transducer with the prescribed optics, the difference between those indicated in Table 3 and those given above for the transducer formats does in some ways establish some specification for the zoom lens requirements. A chosen format established the maximum allowed on the transducer; the desired "last look" before impact establishes the maximum image change factor. The two are reconciled by the demagnification of the zoom lens system. Since the current state of the art for these lenses shows that a 10X magnification can be achieved, we can expect that 10X the values established by transducer limits are the upper limits on the image change factor. Thus, according to whichever value is picked from the above discussion, we could have image change factors of 261, 425, 1440, or 2280 depending upon the format and focal length of the zoom lens. We see from Table 3 that the range from impact potentially will be quite small. However, before the benefits of this optical advantage can be taken, one must also reconcile such important influences as the zoom lens speed of response and the transducer update capability. Only the latter is considered in this report.

An interesting comparison can be obtained from Eq. (3). We can determine the variation in image size for the "near field" scene (i.e., for R^-) and observe the simultaneous change in the "far scene" (i.e., for R^+). This is equivalent to the projectile heading toward a close target and yet, having another target in the field of view also changing. Of course, the latter target would be quickly lost from the scene if the projectile were guided

to the closest target,or it would be lost from the field of view anyway at a later time as the areal ground coverage reduces as the projectile approaches impact. In either case, we can observe how the relative image change factors for both scenes are altered, remembering that one scene is lost as time in flight progresses. These comparisons are shown in Figures 6 and 7 for the velocities 214 and 305 m/sec, respectively.

The correlator operates by storing the tactical scene containing the target and then playing the scene through the memory bank, one element of which contains the target to the same scale. Each time the transducer recording is made, it is anticipated that a matched filter has been recorded to the same scale and can be comparable to the input image. Considereing then the foregoing results, we can see that there are significant size changes which must be accounted for. Since each comparison is done in a discrete sequence, we must determine how often an individual scene is recorded, and what change in image size is allowable before the individual scene is recorded. First, we determine how many images are required in the memory.

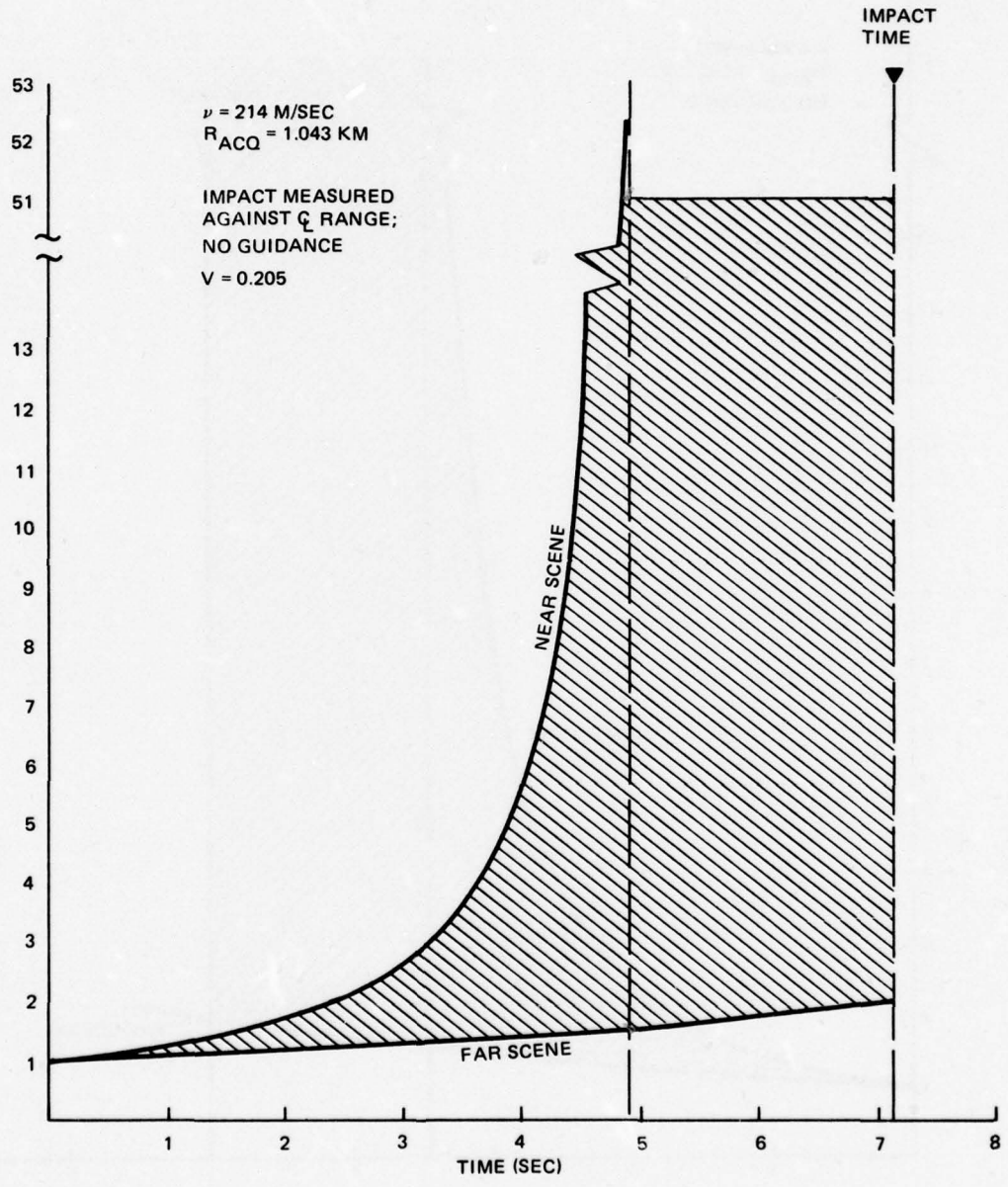

Fig. 6 Image Changes as a Function of Time for Target Position in Scene (V = 0.21)

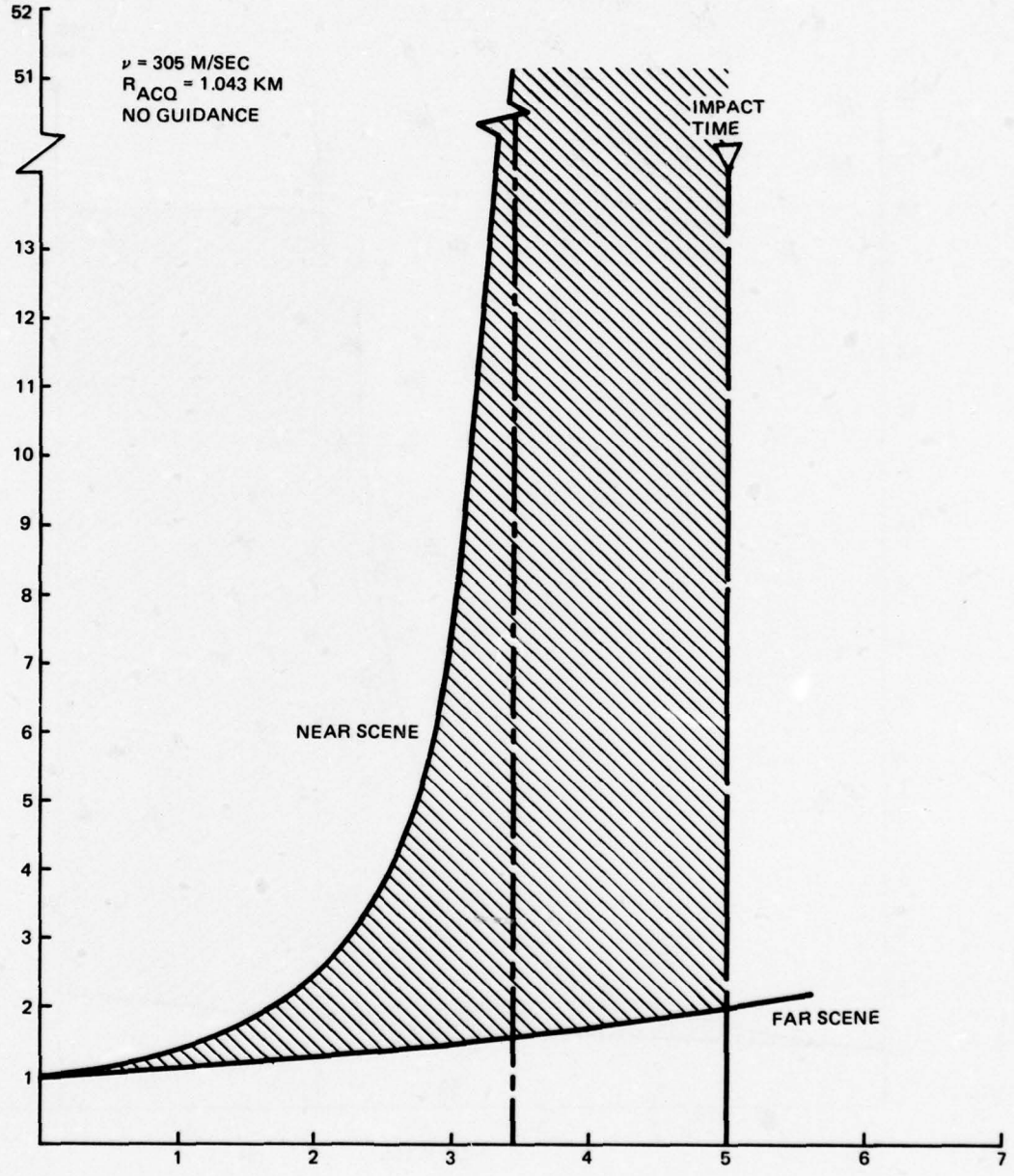

Fig. 7 Image Changes as a Function of Time for Target Position in Scene (V = 0.29)

5. OPTICAL MEMORY BANK REQUIREMENTS

The memory density requirements depend upon the image size change factor, the rate at which update can be achieved, and the parametric sensitivity that is employed for the target image. At least one experience (Ref. 6) has shown that the (-3dB) scale sensitivity variation is ± 20 percent (area) for the M-60 in an overhead view. The linear scale variation for the 100 percent minimum image then becomes 1.0 ± 0.1. We can determine the linear (scale) size factor, F, for any variation, that prudence or experimental results dictate, from the fact that the upper limit for one matched filter is the lower limit for the adjacent one. Thus,

$$F = \left(\frac{1 + \alpha}{1 - \alpha} \right)^N \tag{4}$$

where N = 0, 1, 2, ... is the number of filters required in order to achieve a linear size factor of F when a (symmetrical), -3dB parametric sensitivity is ± α. The coefficient N must, of course, be an integer, and it represents the whole number of matched filters needed to achieve a linear size factor of F. Allowing only then for a scale change in the target size, we can compute the number of filters required for any scale (expressed relative to theinitial size). This is summarized in Table 5 for a ± 10 percent scale change, -3dB sensitivity. We can carry this analysis further and consider the requirements that a scale change, with full azimuthal coverage for each scale, would demand.

The criteria for the allowance for orientation variations are also derived from Ref. 6. Although the data are based upon a strategic, or overhead view, and the present application requires

an oblique one, the data to be used are believed to be valid. This is based upon an unpublished investigation which showed that the average sensitivities of a matched filter to variations about an oblique view of the (tank) target are comparable. This means that head-on views were more sensitive but side views less sensitive. Thus, the assumption of $\pm 8^{o}$ seems to be a reasonable one.

TABLE 5 NUMBER OF FILTERS REQUIRED FOR $\pm$ 10 PERCENT SCALE CHANGE SENSITIVITY

Scale Size F	Number of Matched Filters Required N
1	1
2	4
3	6
4	7
5	9
6	10
7	10
8	11
9	12
10	12
15	14
20	16
25	17
30	18
35	18
40	19

If we now assume that (1) there is no interaction between the parameters scale and orientation, and (2) the orientation sensitivity is a constant regardless of the actual scale, then the number of required filters can be obtained from Eq. (4) and a consideration for projectile velocity. Thus

$$\text{No. of Filters Required} = W\left[\frac{\log F}{\log\left(\frac{1+\alpha}{1-\alpha}\right)} + 1\right] \qquad (5)$$

where all the quantities are as previously given and W = 360/ (orientation sensitivity fullwidth) taken to the next highest whole number. For $\pm 8^{o}$, W = 23.

The number of filters required for $\alpha = \pm 0.1$, $\theta = \pm 8^{o}$ has been computed, and is, of course, dependent only upon the parametric sensitivities and the largest value of F allowed. The results for the case cited are given in Table 6. These results are a more realistic estimate since target placement and size have been accounted for.

It can be seen that many positions of optical memory are required for representative tolerances in the parameters. However, it has been previously shown (Ref. 6) that recording 128 filter positions on an area of 40 x 40 mm is not beyond the state of the art. Through such techniques as overlay and interlace this number can be increased to 500. Also, the filter capability cited is based upon a given transform lens focal length (360 mm). Decreasing this would increase the storage capability by a factor $(360/\text{new FL})^2$ for the same area. For example, we could obtain an increase in storage capacity by about a factor of 4 and still be above the storage medium's limiting resolution. Thus, the seemingly large value of 397 is well within the bounds of current

TABLE 6 NUMBER OF FILTERS REQUIRED FOR SCALE CHANGE OF ± 10 PERCENT AND ORIENTATION SENSITIVITY OF ± 8°

Linear Size Factor	Whole Filters Required
1	23
2	103
3	149
4	182
5	208
6	229
7	247
8	262
9	275
10	287
11	298
12	308
13	318
14	326
15	334
16	341
17	348
18	355
19	361
20	367
21	372
22	378
23	383
24	388
25	392
26	397

technology. It should be pointed out, however, that the task of preparing that number of memory positions is time consuming and tedious. The ameliorating factor is that usually only one filter is required and that photographic replication (for many projectiles) might be possible.

It has also been shown that the degree of discrimination exhibited by a matched filter depends upon the order of the filter and that parametric sensitivities generally associate with filter order. Thus, some degree of parametric latitude should be accounted for. This has been done by using Eq. (4) and allowing α and W to assume the values 0.05, 0.10, 0.15, 0.20, and $\pm 8^{\circ}$, $\pm 10^{\circ}$, $\pm 12^{\circ}$, respectively. A few selected results are shown in Table 7 for the size factors F = 26.1, a value obtained from the transducer format filling consideration given in Table 4. Similar results could be computed for other filling factors.

TABLE 7 NUMBER OF MATCHED FILTER MEMORY ELEMENTS REQUIRED FOR VARIOUS SCALE AND ORIENTATION SENSITIVITIES (MAXIMUM IMAGE TO FILL TRANSDUCER)

Scale Parametric Sensitivity	Number of Filters Required for a -3 db Width of		
	$\pm 8^{\circ}$	$\pm 10^{\circ}$	$\pm 12^{\circ}$
0.05	772	604	504
0.10	397	311	259
0.15	271	213	177
0.20	208	163	136

The results of Table 7 clearly indicate that OMFIC memory requirements are a manageable factor in the system concept. This is particularly so when the tactical requirement calls for zeroing

in on a class of vehicles (e.g., tanks) rather than a specific one (e.g., M-60 versus M-48). The next task is to determine how often, and how fast, the transducer must be recycled in order to meet the requirements dictated by the foregoing results.

6. DETECTOR RESPONSE-TIME CONSTRAINTS

It is apparent now that one of the unique problems associated with the guidance of projectiles in a terminal homing mission is the change of target size in a fixed focus imaging sensor. If we assume that the final detector is located in the correlation plane, i.e., it detects the peak correlation between the target being viewed and the target image in memory, then we must contend with the fact that the peak correlation signal will vary with the size or scale of the incoming image. One way to avoid the impact of the problem is to arrange perfect registration of the correlation signal from all the target sizes from the different positions in the matched filter memory onto a common correlation plane. However, if we lost registration or if we elect for signal-to-clutter considerations to have separate correlation plane detection for each memory location then we must consider the time variation of an individual matched filter which was made for a fixed range interval. Since we must sense the peak signal, this would impose a constraint on the response time of the detector. We assume in this section that the image presented to the matched filter or correlator has not been smeared by any other components such as the electro-optic transducer that converts the input incoherent image into a coherent image. This is the case when the response time of the transducer is fast enough; the burden then falls on the detection plane. A corresponding analysis of the effects of image scale size charge is given later in this report to address the other alternative, i.e., where the transducer becomes the limiting component.

If we assume that the target is imaged by a fixed aperture lens, and the projectile is moving with velocity v then the linear image size can be expressed as (see Eq. (3)):

$$\frac{\ell}{\ell_o} = \frac{1}{(1-\frac{vt}{R})} = \frac{1}{\alpha} \tag{6}$$

where ℓ_o is the image size where the range to the target is R and the elapsed time from acquisition t equals zero. We note that if the image formed by the sensor at time t = 0 is expressed as f(x,y), where x and y are coordinates in the image plane and f is the optical amplitude (the intensity in watts/cm^2 being given by the square of f), then as the image changes size its optical amplitude will change. If we assume that the sensor has a fixed aperture and that the light propagation can be computed on a spherical wave basis, then the intensity I_i at a given point in the image plane is given by

$$\frac{I_i}{I_s} = \frac{1}{(f/A)^2} = \frac{1}{(f/\#)^2} \tag{7}$$

where I_s is the intensity of the equivalent point source, F is the focal length of the system, A is the linear dimension of the aperture, and (f/#) is the so called f-number of the lens. For a fixed lens we see that the point-by-point image intensity is not a function of range to the target; we will refer to this as the fixed intensity model. Then as the image size changes the image simply expands or contracts so that the optical amplitude of the image is given by $f(\alpha x, \alpha y)$ with $\alpha = 1-vt/R$. If, on the other hand, we assumed that the light propagation from the target is not spherical with a $(1/R^2)$ intensity fall off then we must consider a variable intensity of the image. To bracket our results we will consider the case where the total light flux in the image remains constant as the image changes size. This then requires that the image intensity decrease as the image grows

larger to keep the total light flux constant. This case yields our optical amplitude given by α f(x,y) so that the integral of the optical intensity

$$\int\int \alpha^2 f^2(\alpha x, \alpha y)\, dxdy = \int\int f^2\,(r,s)\, drds = \text{constant} \quad (8)$$

remains the same as the image changes size (or α changes).

The matched filtering or correlation operations on the sensed image will be written as

$$C(\xi,\eta) = \int\int g(x,y)\; h(x+\xi,\; y+\eta)\; dx,dy \quad (9)$$

where g is the sensed image (either $f(\alpha x,\alpha y)$ or $\alpha\, f(\alpha x,\alpha y)$ depending upon the nature of the imaging system) and h (x,y) is the matched filter. We will consider high pass matched filters in the present discussion so that h(x,y) is a high pass replica of the given image f(x,y) that is selected at some nominal scale, say $\alpha = 1$. In order to obtain specific results we will take a simple rectangular figure as the prototype f(x,y), i.e.,

$$f(x,y) = \begin{cases} 1 & , \; |x| \le \frac{L_x}{2} \;,\quad |y| \le \frac{L_y}{2} \\ 0 & \text{elsewhere} \end{cases} \quad (10)$$

In this case we may express the peak value of the correlation signal $C(\xi,\eta)$ as (for example in the fixed intensity model)

$$C_p = C(0,0) = \int\int g(x,y)\; h(x,y)\; dx,\; dy$$

$$C_p = C(0,0) = \iint f(\alpha x, \alpha y)\ f_{HP}(x,y)\ dx\ dy$$

$$= \iint f(\alpha x, \alpha y)\ f(x,y)\ dx\ dy -$$

$$\iint f(\alpha x, \alpha y)\ f_{LP}(x,y)\ dx,\ dy \qquad (11)$$

where f_{HP} and f_{LP} refer to the responses of the high pass and low pass matched filters, respectively. In particular, we find that that if $\alpha < 1$ then for the simple rectangular figure

$$\iint f(\alpha x, \alpha y)\ f(x,y)\ dx\ dy = \iint f^2(x,y)\ dx\ dy = L_x L_y \qquad (12)$$

and

$$\iint f(\alpha z, \alpha y)\ f_{HP}(x,y) dx dy = \frac{1}{(2\pi)^2} \iint \mathcal{J}[f(\alpha x, \alpha y)]$$

$$\mathcal{J}\ [f_{LP}(x,y)]\ dx\ dy \qquad (13)$$

where $\mathcal{J}(\cdot)$ denotes the two-dimensional Fourier transforms. Using the fact that

$$g\ [f(\alpha x, \alpha y)] = \frac{1}{\alpha^2}\ \ F\ \left(\frac{\omega_x}{\alpha}\ ,\ \frac{\omega_y}{\alpha} \right) \qquad (14)$$

we then have

$$\iint f(\alpha x,\alpha y)\, f_{LP}(x,y)\,dxdy = \frac{1}{(2\pi)^2}\,\frac{1}{\alpha^2}\int_{-B_y}^{B_y}\int_{-B_x}^{B_x}\left(\frac{2\,\mathrm{Sin}\,\frac{\omega_x L_x}{2\alpha}}{\frac{\omega_x}{\alpha}}\right)\left(\frac{2\,\mathrm{Sin}\,\frac{\omega_y L_y}{2\alpha}}{\frac{\omega_y}{\alpha}}\right)\cdot \tag{15}$$

$$\left(\frac{2\mathrm{Sin}\,\frac{\omega_x L_x}{2}}{\omega_x}\right)\left(\frac{2\mathrm{Sin}\,\frac{\omega_y L_y}{2}}{\omega_y}\right) d\,\omega_x\, d\,\omega_y$$

where we have used the Fourier transform of the rectangle and defined B_y, B_x to be the frequency of the filter. If we then form a "figure of merit" function P given by the ratio of the square of the peak correlation function at various scales or α's to the square of the peak correlation function at $\alpha = 1$ we have, after simplification

$$P_F = \alpha^2 \left[\frac{1 - \frac{16}{\pi^2} A_1A_2}{1 - \frac{16}{\pi^2} A_3A_4}\right] \tag{16}$$

in the fixed image flux model and

$$P_F = \left[\frac{1 - \frac{16}{\pi^2} A_1A_2}{1 - \frac{16}{\pi^2} A_3A_4}\right]^2 \tag{17}$$

in the fixed image intensity model, where

$$\left.\begin{aligned} A_1 &= \frac{1}{2}\int_0^{\frac{B_x L_x}{2}} \frac{\operatorname{Sin}\frac{r}{\alpha}\operatorname{Sin} r}{r^2}\,dr, \qquad A_2 = \frac{1}{2}\int_0^{\frac{B_y L_y}{2}} \frac{\operatorname{Sin}\frac{r}{\alpha}\operatorname{Sin} r}{r^2}\,dr \\ A_3 &= \frac{1}{2}\int_0^{\frac{B_x L_x}{2}} \frac{\operatorname{Sin}^2 r}{r^2}\,dr, \qquad A_4 = \frac{1}{2}\int_0^{\frac{B_y L_y}{2}} \frac{\operatorname{Sin}^2 r}{r^2}\,dr \end{aligned}\right\} \quad (18)$$

We have computed a series of curves to indicate the expected variation of the performance function P with various image scales in the case where $L_y = 2L_x$ and $B_x = B_y = B$. Figure 8 shows the results for the fixed intensity case P_I; note the very rapid changes as the normalized cutoff frequency $\frac{B_x L_x}{2} = \frac{BL_x}{2}$ varies from $\pi/4$ to π in Figures 8(a) and 8(b), and then the saturation effect as we go to values as large a 5π in Figure 8(c). In order to illustrate the nature of the effect we also computed the value of the image scale change that would produce a performance function value of 1/2, at different values of cutoff frequency. In order to ease this calculation we assumed that this would occur at values of α near 1 so that we could write, for example, $\alpha = 1 - \epsilon$ and

$$\operatorname{Sin}\frac{r}{2\alpha} \approx \operatorname{Sin}\frac{r}{2} + \frac{r\epsilon}{2}\operatorname{Cos}\frac{r}{2} \quad (19)$$

In this case we have, continuing the first order analysis

$$P_I = (1 - k\epsilon)^2 \quad (20)$$

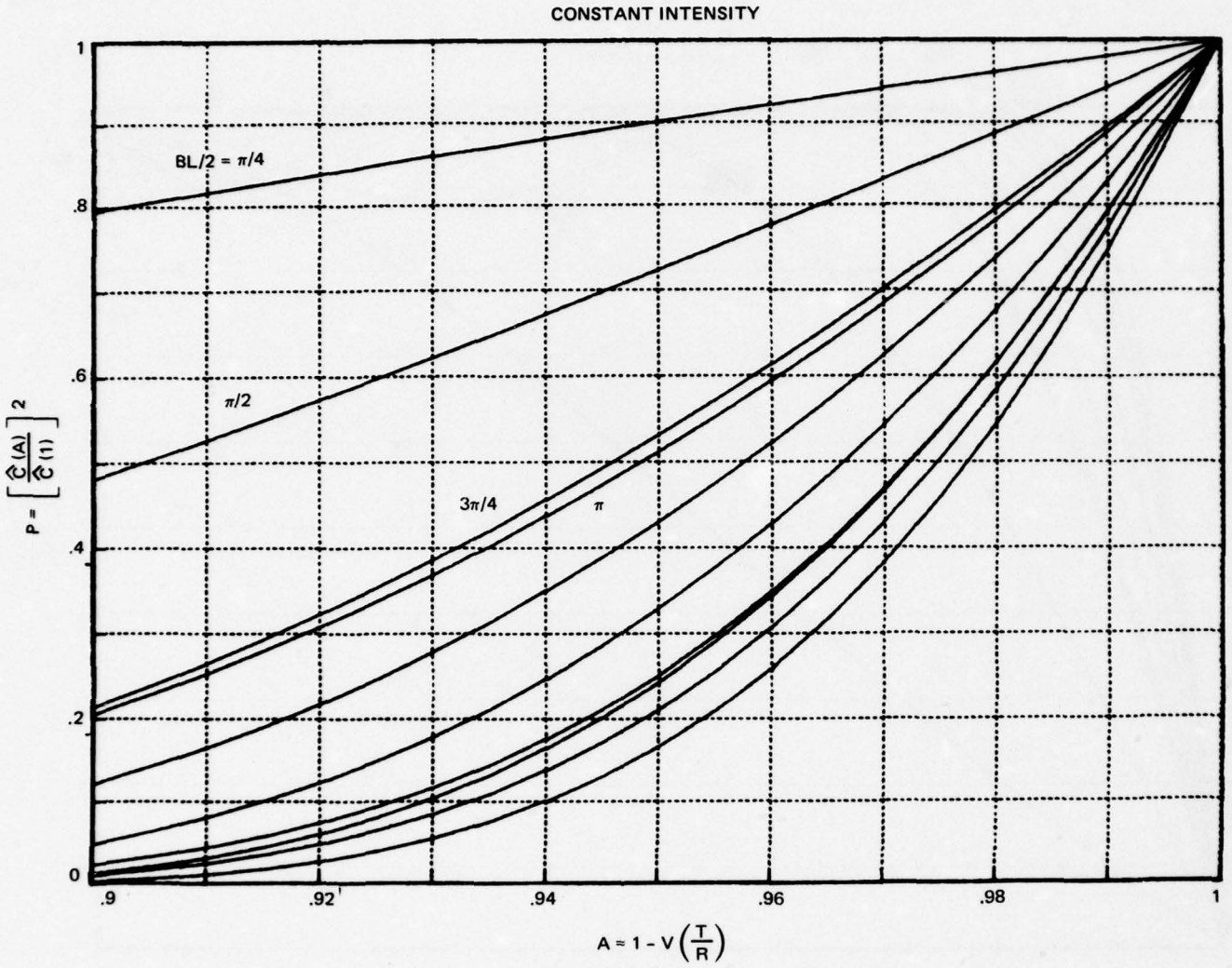

Fig. 8a Variation of Correlation Signal Due to Image Scale (A) for Constant Image Intensity and Various Cutoff Frequencies ($\frac{BL}{2}$). ($\frac{BL}{2}$ from $\pi/4$ to 2.5π in $\pi/4$ steps)

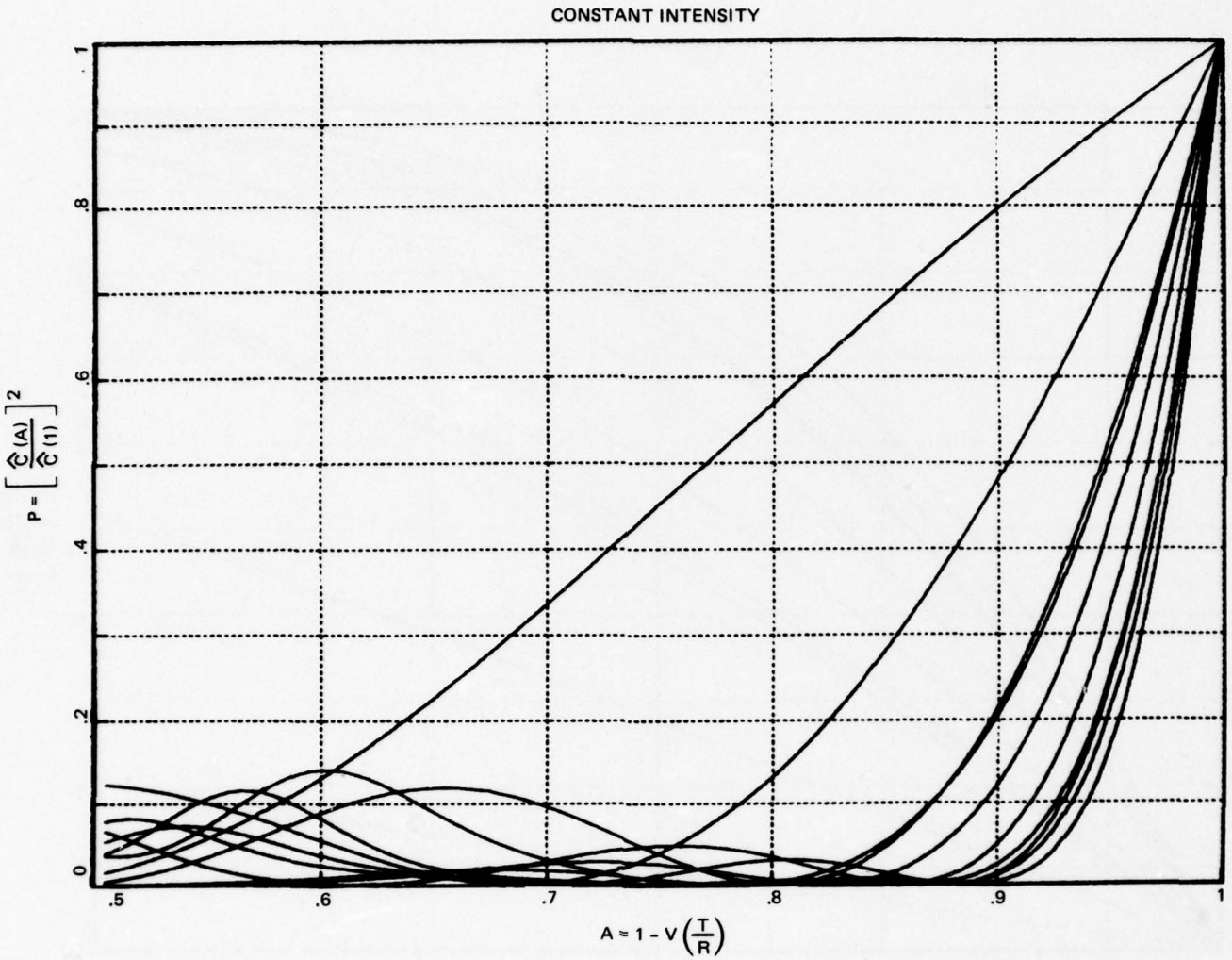

Fig. 8b Variation of Correlation Signal Due to Image Scale (A) for Constant Image Intensity and Various Cutoff Frequencies ($\frac{BL}{2}$). ($\frac{BL}{2}$ from $\pi/4$ to 2.5π in $\pi/4$ steps (expanded scale))

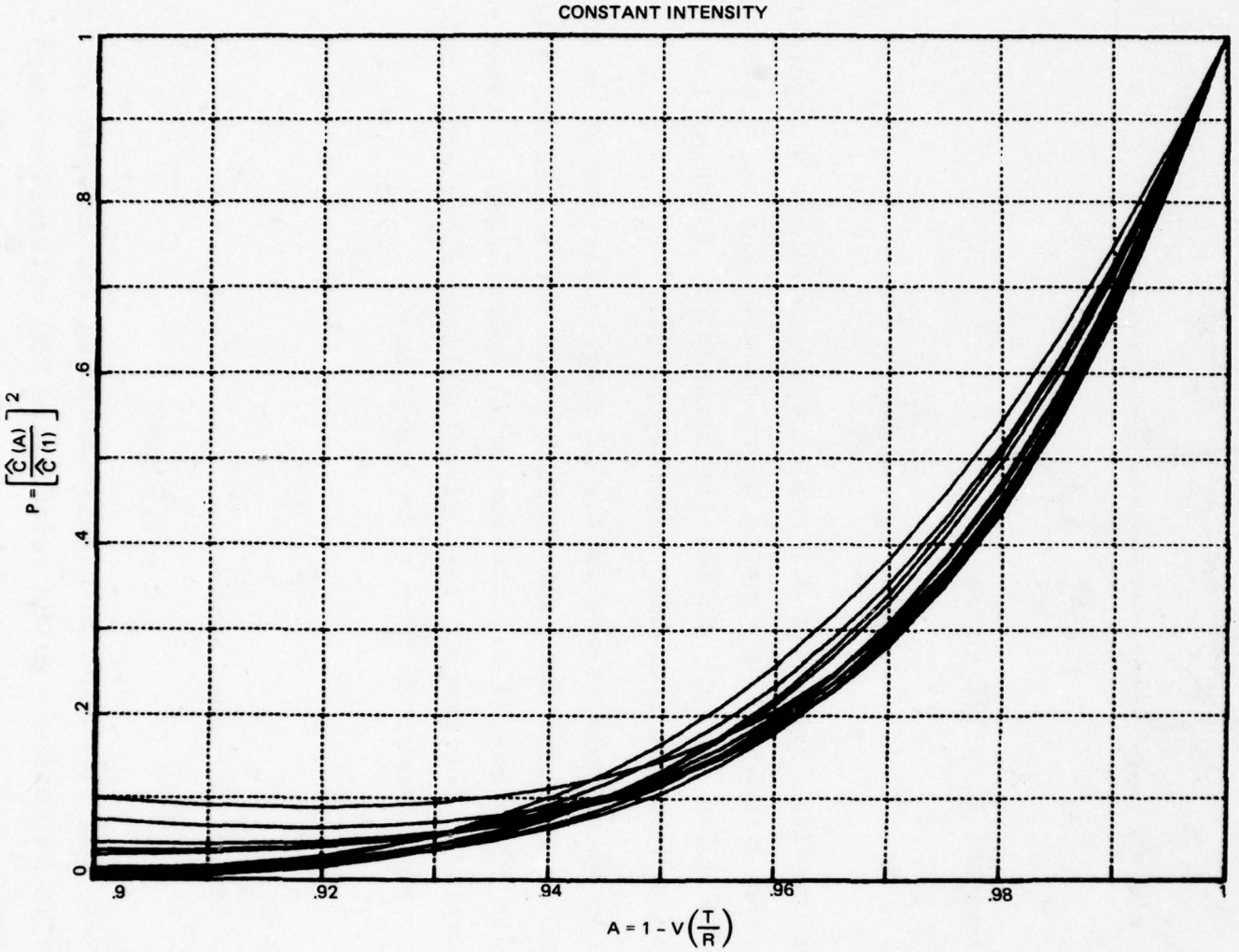

Fig. 8c Variation of Correlation Signal Due to Image Scale (A) for Constant Image Intensity and Various Cutoff Frequencies $(\frac{BL}{2})$. ($\frac{BL}{2}$ from 2.5 π to 4π in $\pi/4$ steps)

where

$$K = \frac{4}{\pi^2} \frac{A_3 \int_0^{BL_y} \frac{\text{Sin}r}{r}\, dr + A_4 \int_0^{BL_x} \frac{\text{Sin}r}{r}\, dr}{1 - \frac{16}{\pi^2} A_3 A_4} \tag{21}$$

and we have $P_I = 1/2$ where

$$\epsilon = \frac{vt}{R} = \frac{1 - \frac{1}{r^2}}{k} \tag{22}$$

These results, for $\left|\frac{vt}{R}\right| < 0.1$ are plotted in Figure 9 together with the corresponding results where we consider the fixed flux model for the sensor. We see the saturation effect as the normalized cutoff frequency goes beyond 2π.

As an example of the impact of image scale change on the system -- consider the case where V = 300 meters/sec (Mach 1) and R = 10 meters, i.e., the sensor is operating at a range of 10 meters to the target; then if we utilized a high pass matched filter with bandwidth $\frac{BL}{2} = \pi$, we would have

$$\frac{vt}{R} = 0.05$$

for a fixed intensity sensor or

$$t = 1.7 \text{ msec}$$

However, the situation is highly variable; for example, if the range is 50 meters and the velocity is 150 meters/sec (Mach .5) we have T = 17 msec to read the correlation signal before it falls to 1/2. That is, when the projectile is 50 meters from the target, it takes 17 msec for the output correlation signal power to drop by a factor of 1/2 and this would imply the need to have a detector response faster than 17 msec.

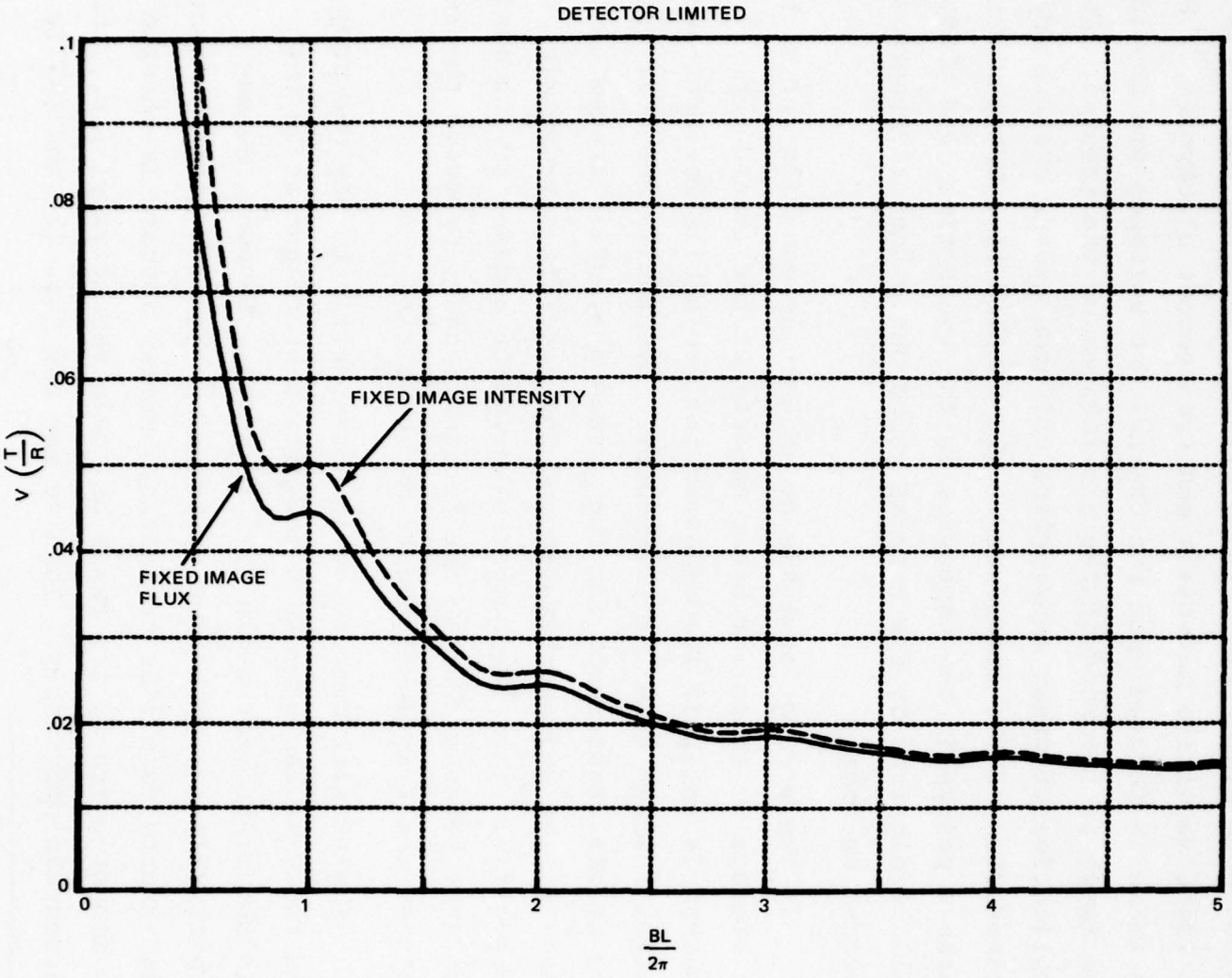

Fig. 9 Elapsed Time (VT/R) Before Peak Correlation Signal Drops by 1/2 Due to Image Scale Change for Various High Pass Filter Cutoff Frequencies (BL/2π)

7. TRANSDUCER UPDATING REQUIREMENTS

The transducer is an image storing device consisting of an anisotropic dielectric, liquid crystal contained between layers of light sensitive materials and transparent electrodes.* When an image is focused upon the crystal and voltages are applied, the image is recorded in the alterations of the crystal. The application of other appropriate voltages causes erasure and restoration of the transducer. The elapsed time between comparable points in the exposures is the cycle time, and this time will be dictated by the rate at which one wishes to record and process an image.

In the present analysis no account is made for the mechanics of storage or erase, or other aspects of the transducer. The concern is entirely focused upon the projectile movement and the target's image upon the transducer. Eventually one must establish the update requirement for the guided projectile system on the basis of the guidance system and the specific aerodynamics of the projectile. Thus the number of guidance updates or the minimum distance between them in the terminal phase, produces the requirement as the transducer update or cycle time.

The present discussion is not specific to any one projectile and thus, we cannot make a definitive statement as to the minimum transducer cycle time required. However, we may arbitrarily set this time by assuming that the guidance system will update each time the optical memory address is changed by an amount given by its range or scale sensitivity, i.e., the α's introduced previously. Then we may use Eqs. (3) and (4) to

---

* The discussion applies to the transducer described in Refs. 4 and 5; a similar transducer is described in Ref. 10 and the reference cited therein. Other transducers are described in Ref. 11.

establish the minimum time corresponding to the last update at a fixed scale factor change. Equating the two equations leads to

$$t = \frac{\left(\frac{1+\alpha}{1-\alpha}\right)^N - 1}{\left(\frac{1+\alpha}{1-\alpha}\right)^N V} \tag{23}$$

where as before $V = v/R$.

Equation (23) has been computed for the sequence of V-values for the scale sensitivity increments $\alpha = 0.05$, 0.10, 0.15 and 0.20 for two cases. The first is for times quite close to impact and the second, for the case where the transducer is updating at close to television frame rates.

The results for the first case are summarized in Table 8, as we see there is a requirement for update rates that can be an order of magnitude faster than TV frame rates. The columns 3-5 and 6-8 show, respectively, the elapsed time and the duration of the update interval for the case where $N = 1$, and the case where the elapsed time is close to the impact time shown in column 9.

Several conclusions emerge from Table 8. Not surprising, the higher V is, the shorter the update interval must be although it can also be seen that the scale parametric sensitivity can be traded off for velocity ratio. In fact, the least sensitive filter operated $V = 0.38$ requires the same time to cycle as the most sensitive filter at low velocity. This comparison is significant when we consider that for the centerline acquisition range $R_o = 1.525$, $V = 0.38$ implies a projectile flying at Mach 1.7.

For the more realistic ratios $V = 0.14$, 0.20 the transducer update interval average is about 7.5 msec. This is about an

TABLE 8 TRANSDUCER UPDATE REQUIREMENTS

Velocity Ratio (v/R)	Parametric Sensitivity Increment (α)	F (Low)	Elapsed Time (sec)	Update Interval (sec)	F (High)	Elapsed Time (sec)	Update Interval (Millisec)	Impact Time t_I (sec)
0.14	0.05	1.11	0.68	0.62	149	7.10	4.56	7.14
	0.10	1.22	1.30	1.06	184	7.10	7.04	
	0.15	1.35	1.86	1.38	170	7.10	10.93	
	0.20	1.50	2.38	1.59	195	7.11	12.23	
0.20	0.05		0.47	0.43		4.97	3.19	5.00
	0.10		0.90	0.74		4.97	4.93	
	0.15		1.30	0.96		4.97	7.65	
	0.20		1.67	1.11		4.97	8.56	
0.26	0.05		0.37	0.33		3.82	2.45	3.85
	0.10		0.70	0.57		3.83	3.79	
	0.15		1.00	0.74		3.83	4.35	
	0.20		1.28	0.85		3.83	6.59	
0.32	0.05	SAME	0.30	0.27	SAME	3.10	1.99	3.13
	0.10		0.57	0.46		3.11	3.08	
	0.15		0.82	0.60		3.11	4.78	
	0.20		1.04	0.69		3.11	5.35	
0.38	0.05		0.25	0.23		2.61	1.68	2.63
	0.10		0.48	0.39		2.62	2.59	
	0.15		0.69	0.51		2.62	4.03	
	0.20		0.88	0.58		2.62	4.51	

order of magnitude shorter than current technology allows for low light illumination of the transducer. For bright sunlight, recording times of 6 msec have been demonstrated.

The results of the second case — which might be called the current technology case — are summarized in Table 9. The column headings are similar to those of Table 8 except that an additional column has been added to show the range from the target. These data are significant because they show that except for one case ($V = 0.38$, $\alpha = 0.05$) the transducer performance is sufficiently satisfactory to update to a point quite close to the target. Except for the two extreme speeds ($V = 0.32$, 0.38) this distance is $d \lesssim 100$ meters and therefore, the question as to where the last guidance update is given becomes pertinent and must be examined.

Shown in column 7 is the range "bin" interval which is covered by the memory position (-3dB coverage) corresponding to the parametric sensitivity increment, α. The intervals, of course, vary in proportion to the absolute distance from impact.

TABLE 9 TRANSDUCER UPDATE REQUIREMENTS - CURRENT TECHNOLOGY

Velocity Ratio (v/R)	Parametric Sensitivity Increment (α)	N	Elapsed Time (sec)	Update Interval (ms)	Range From Target (M)	Range "Bin" Interval (M)	Impact Time (sec)
0.14	0.05	31	6.82	30.54	67	64 - 70	7.14
	0.10	19	6.99	28.69	32	29 - 35	
	0.15	14	7.04	27.04	21	18 - 24	
	0.20	11	7.06	27.53	17	14 - 20	
0.20	0.05	27	4.67	31.91	100	95 - 105	5.00
	0.10	17	4.83	30.00	51	46 - 56	
	0.15	13	4.90	25.64	30	26 - 35	
	0.20	10	4.91	28.90	27	22 - 32	
0.26	0.05	27	3.59	24.55	100	95 - 105	3.85
	0.10	16	3.69	28.21	62	56 - 68	
	0.15	12	3.74	26.68	43	37 - 49	
	0.20	9	3.75	33.35	39	31 - 47	
0.32	0.05	23	2.81	29.77	154	146 - 162	3.13
	0.10	15	2.97	28.01	77	69 - 85	
	0.15	11	3.01	29.33	48	41 - 55	
	0.20	9	3.04	27.10	43	34 - 52	
0.36	0.05	23	2.37	25.07	206	196 - 216	2.63
	0.10	14	2.47	28.83	91	82-100	
	0.15	10	2.50	33.42	74	63-85	
	0.20	8	2.53	34.23	57	46 - 68	

8. IMAGE ENLARGEMENT SMEAR - CONSTRAINTS IMPOSED ON TRANSDUCER RESPONSE TIME

During projectile flight the duration of exposure for recording the image on the transducer is comparable to that for photographic exposures in aerial reconnaissance cameras. It is anticipated however, that the guided projectile may not have the benefit of image motion compensation (IMC) -- now a standard approach in cameras. Also, one cannot rely upon post facto removal of motion degradations because of the real time nature of the application. Thus, some measure of image motion degradation might be anticipated.

In aerial cameras, the degradation usually takes the form of a linear image motion, defocus or vibration, and occasionally enlargement smear. In the OMFIC-GP application it is anticipated the principal cause of smearing will be the latter. While the presence of other degradations might be explored for an implemented OMFIC-GP, enlargement smear is expected to be present and the only one considered here.

If a zoom lens system is employed as indicated in the schematic of Figure 3, it is interesting to contemplate the possibility of achieving compensation through incremental zoom-lens control. However, this implementation problem is not examined here although the results of this analysis might be useful in the analysis for image correction through a zoom lens.

We can use Eq. (2) in a modified form. If we consider the instantaneous image rather than the acquisition image size on the transducer, we can then interpret the image as the "acquisition image" when the shutter is open. The left hand side of Eq. (2), designated $\mathcal{L}$, represents the image change while the shutter is

open. Taking differentials of ℓ and t, dividing by the image size when the shutter is open, I_s, we obtain

$$S = \frac{\Delta\ell}{I_s} \times 100 = V\left[\frac{1}{(1 - Vt)^2}\right]\Delta t \times 100 \qquad (24)$$

$$= \% \text{ Enlargement Smear}$$

Equation (24) has been computed and the results are shown in Figure 10 for two velocity ratios (0.14 and 0.26) and for exposure times of 10 and 50 msec. The last two values were chosen because they bracket anticipated and current transducer technology. Actually, the former value can also be achieved although the illumination requirements call for bright sunlight.

It is not surprising that the shorter exposure results in less smear, nor that near impact the smear is greatest. The latter follows from the results described in Section 4 which showed the rapid growth in image size near impact.

If IMC is to be achieved through the zoom optical system, it is clear that it must be coordinated well with the system, record/read cycle, and have millisecond reaction times.

In the remainder of this section we will evaluate the effect of uncompensated scale change on the correlation signal obtained with a fixed target image when an incoherent-to-coherent optical transducer is present. The basic effect of the transducer will be to smear the input or sensor image since the time interval necessary for the transducer to produce sufficiently intense images might be so long that we would have to consider the change of image size during the exposure time. In this sense, the transducer is acting like film that is recording an image whose size changes during exposure resulting in a blurred or smeared

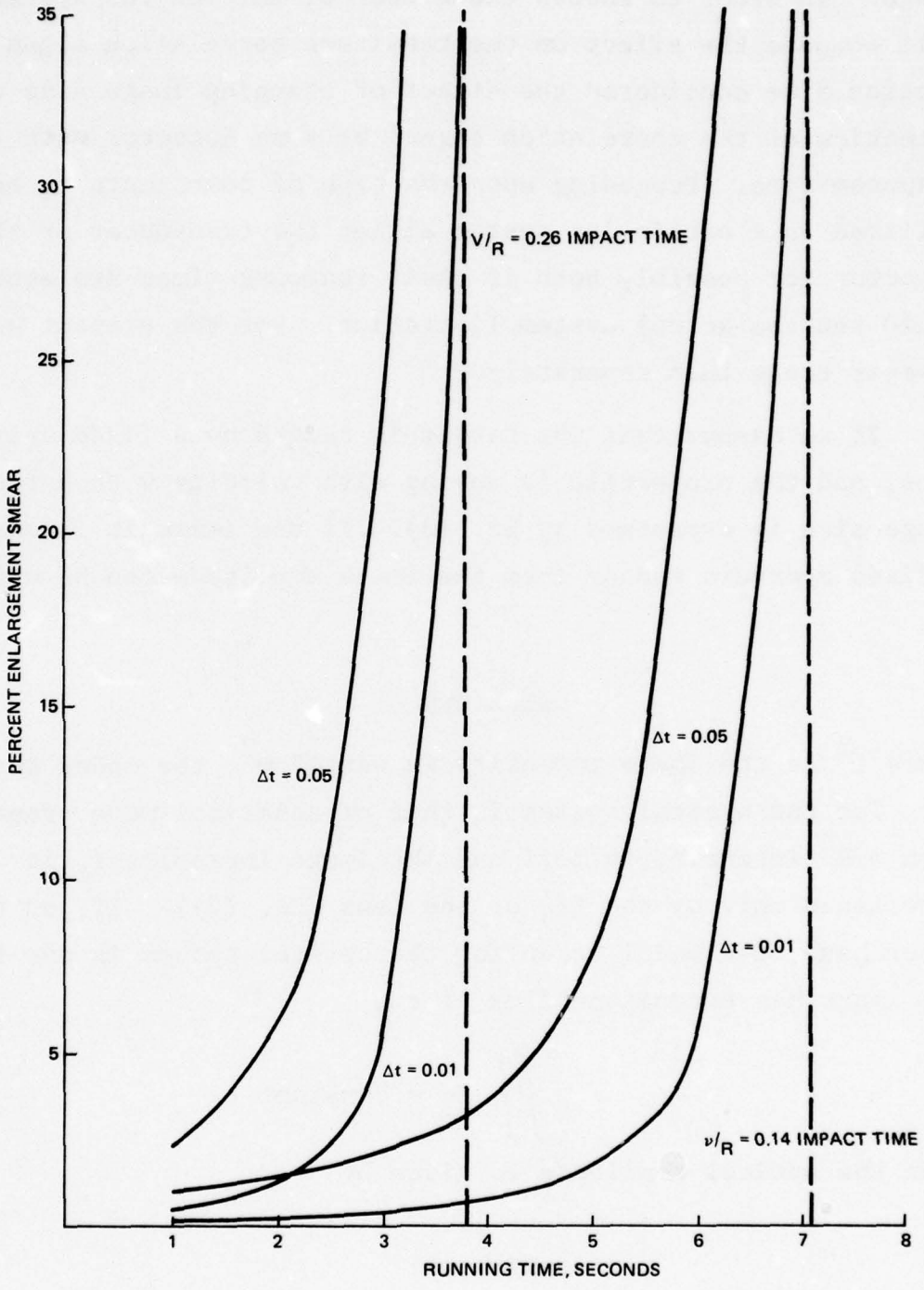

Fig. 10 Enlargement Smear as a Function of Flight Time for Two Velocity Ratios

image. In order to assess the effect of this on the system we will compute the effect on the resultant correlation signal. In Section 5 we considered the effect of changing image size on the detection of the correlation signal by some detector with limited response time. Depending upon the type of components to be utilized in a particular system either the transducer or the detector (or possibly both if their response times are equivalent) could set the actual system limitation. For the present we will however treat them separately.

If we assume that the target is imaged by a fixed aperture lens, and the projectile is moving with velocity v then the linear image size is expressed by Eq. (3). If the image is formed by a fixed aperture sensor then the image amplitude can be written as

$$f(\alpha x, \alpha y) \tag{25}$$

where f^2 is the image intensity in watts/cm^2; the model assumed here for the optical system is that of spherical wave propagation with $1/R^2$ intensity falloff and the image intensity I_i is determined only by the f/# of the lens (Eq. (7)). If, on the other hand, the model taken for the optical system is one in which the image has a constant flux, i.e.,

$$\iint I_i = \text{constant} \tag{26}$$

then the optical amplitude is given by

$$\alpha f(\alpha x, \alpha y) \tag{27}$$

and the integral of the optical density given by Eq. (8).

Now in order to model the transducer we will assume that the resultant transmission of the transducer after exposure is given as some function of the exposure, i.e., the transmission τ is given as some function $G(\cdot)$ of the total optical energy density incident on it

$$\tau = G\left[\int_0^T g(x,y)\ dt\right] \tag{28}$$

where T is the exposure time and $g(x,y)$ is the optical intensity falling on the transducer which is given in the constant flux sensor model by

$$g(x,y) = \alpha^2 f^2(\alpha x, \alpha y) \tag{29a}$$

of in the constant intensity model by

$$g(x,y) = f^2(\alpha x, \alpha y) \tag{29b}$$

In general, we could have an arbitrary functional dependence $G(\cdot)$ but for our purposes we will assume that the image intensity variations are small and we adopt a linearized model obtained by expanding the expression in a power series in $\int_0^T y$;

thus we will use

$$\tau \sim K_o + K_1 \int_0^T g(x,y)\ dt \tag{30a}$$

$$\sim K_o + K_1 \int_0^T \alpha^2 f^2(\alpha x, \alpha y)\ dt \quad \text{(fixed flux)} \tag{30b}$$

$$\tau \sim K_o + K_1 \int_o^T f^2(\alpha x, \alpha y)\, dt \qquad \text{(fixed intensity)} \quad (30c)$$

The matched filtering or correlation operation on the sensed image after it is recorded on the transducer will be given as

$$C(\xi,\eta) = \iint \left[\int_o^T g(x,y)dt \right] h\left((x+\xi),(y+\eta)\right) dxdy \quad (31)$$

where g is given previously and h(x,y) is the matched filter's response. We will consider high pass matched filters in the present discussion so that h(x,y) is a high pass replica of the intensity of the given image f(x,y) that is selected at the initial range R. In order to obtain specific results we will take a simple rectangular figure described in Eq. (8). We also use the peak correlation signal as our detection signal; for example, in the fixed intensity case we will use

$$\hat{C} \equiv c(0,0) = \iint \left[\int_o^T y(x,y)\, dt \right] f_{HP}^2(x,y)\, dx\, dy$$

$$= \int_o^T \left\{ \iint f^2(\alpha x, \alpha y)\, f_{HP}^2(x,y)\, dxdy \right\} dt$$

$$= \int_o^T \left[\iint f^2(\alpha x, \alpha y) \left[f^2(x,y) - f_{LP}^2(x,y) \right] dxdy \right] dt \quad (32)$$

In particular, if we take the situation $\alpha < 1$ we have for the simple rectangular shape

$$\int\int f^2(\alpha x,\alpha y)\ f^2(x,y)\ dxdy = L_x L_y \tag{33}$$

and

$$\iint f^2(\alpha x,\alpha y)\ f^2_{LP}(x,y)\ dxdy = \frac{1}{(2\pi)^2} \int_{-B_y}^{B_y}\int_{-B_x}^{B_x} \left(\frac{2\sin\frac{\omega_y L_y}{2\alpha}}{\omega_y}\right)\left(\frac{2\sin\frac{\omega_x L_x}{2\alpha}}{\omega_x}\right) \cdot \left(\frac{2\sin\frac{\omega_y L_y}{2}}{\omega_y}\right)\left(\frac{2\sin\frac{\omega_x L_x}{2}}{\omega_x}\right) d\omega_x d\omega_y \tag{34}$$

where we have utilized the Fourier transform of the pulse as

$$\mathcal{F}\left[f^2(\alpha x,\alpha y)\right] = \frac{1}{\alpha^2}\ F\left(\frac{\omega_x}{\alpha},\frac{\omega_y}{\alpha}\right) = \frac{1}{\alpha^2}\left(\frac{2\sin\frac{\omega_x L_x}{2\alpha}}{\frac{\omega_x}{\alpha}}\right)\left(\frac{2\sin\frac{\omega_y L_y}{2\alpha}}{\frac{\omega_y}{\alpha}}\right) \tag{35}$$

and defined B_x and B_y to be the cutoff frequency of the filters. If we form a "figure-of-merit" function P given as the ratio of the square of the peak correlation signal of the smeared image at various exposure times T to the square of the peak correlation signal of the constant scale (unsmeared) image at the same exposure time T then we have, after simplification

$$P_F = \left[\frac{\frac{1}{T}\int_0^T \alpha^2\left(1-\frac{16}{\pi^2}A_1A_2\right)dt}{1-\frac{16}{\pi^2}A_3A_4}\right]^2 \tag{36}$$

in the fixed image intensity model, where $\alpha = \frac{vt}{R}$ and the A_i areas previously given in (Eq. (16)).

We have computed a series of curves to indicate the expected variation of the performance function P with various exposure times in the case where $L_y = 2\ L_x$ and $B_x = B_y = B$. Figure 11 shows the results for the fixed intensity case P_I; note the very rapid changes as the normalized cutoff frequency $\frac{B_x L_x}{2} = \frac{BL_x}{2}$ varies from $\pi/4$ to π (Figs. 11a and 11b) and the saturation as the cutoff frequency extends out to values of 5π (Fig. 11c). In order to illustrate the nature of the effect we also computed the values of normalized exposure time $\frac{vt}{R}$ that would produce a performance function value of 1/2 at different values of normalized cutoff frequency $\frac{BL_x}{2}$. To facilitate this calculation we assumed that this would occur at values of α near 1 so that we could write, for example, $\alpha = 1 - \epsilon$ and

$$\text{Sin}\left(\frac{r}{2\alpha}\right) \sim \text{Sin}\left(\frac{r}{2}\right) + \frac{\epsilon r}{2}\,\text{Cos}\,\frac{r}{2} \tag{37}$$

In this case we have (continuing the first order analysis)

$$P_I = \left[1 - k\,\frac{1}{T}\int_0^T \frac{vt}{R}\,dt\right] = \left[1 - \frac{k}{2}\,\frac{vT}{R}\right]^2 \tag{38}$$

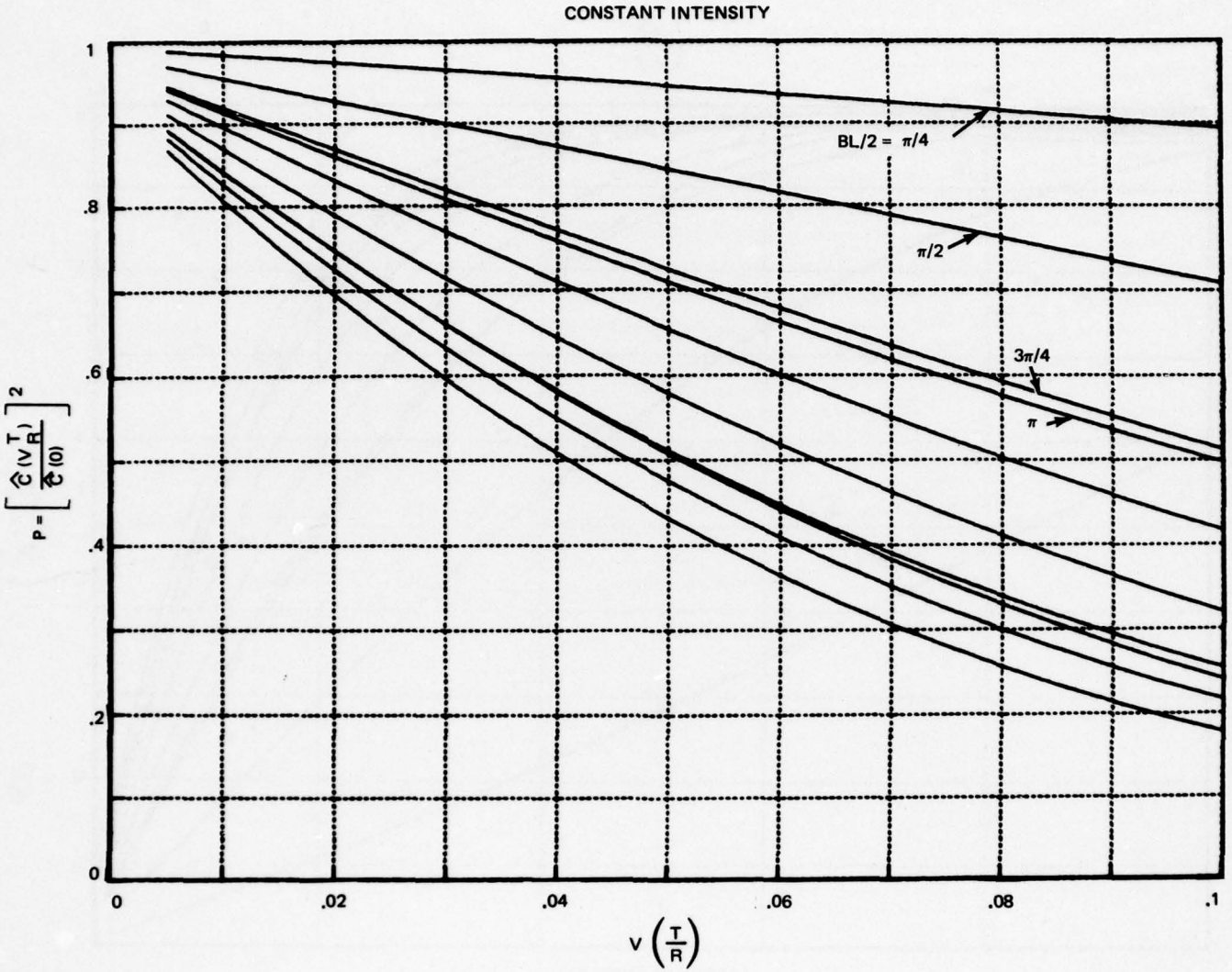

Fig. 11a Variation of Correlation Signal Due to Exposure Time (VT/R) Smearing for Constant Image Intensity and Various Cutoff Frequencies (BL/2). ($\frac{BL}{2}$ from $\pi/4$ to 2.5π in $\pi/4$ steps)

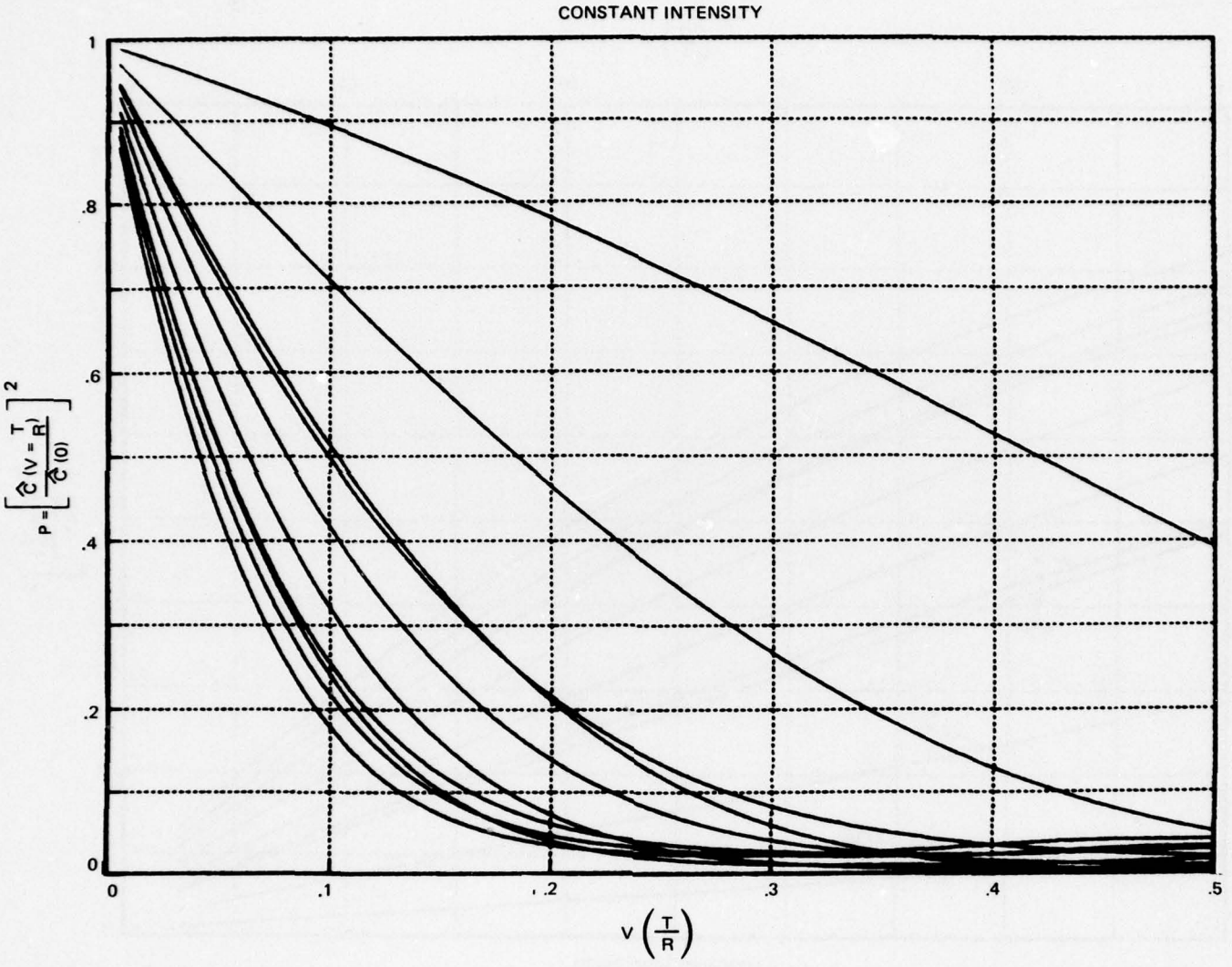

Fig. 11b Variation of Correlation Signal Due to Exposure Time (VT/R) Smearing for Constant Image Intensity and Various Cutoff Frequencies (BL/2). ($\frac{BL}{2}$ from $\pi/4$ to 2.5π in $\pi/4$ steps (expanded scale))

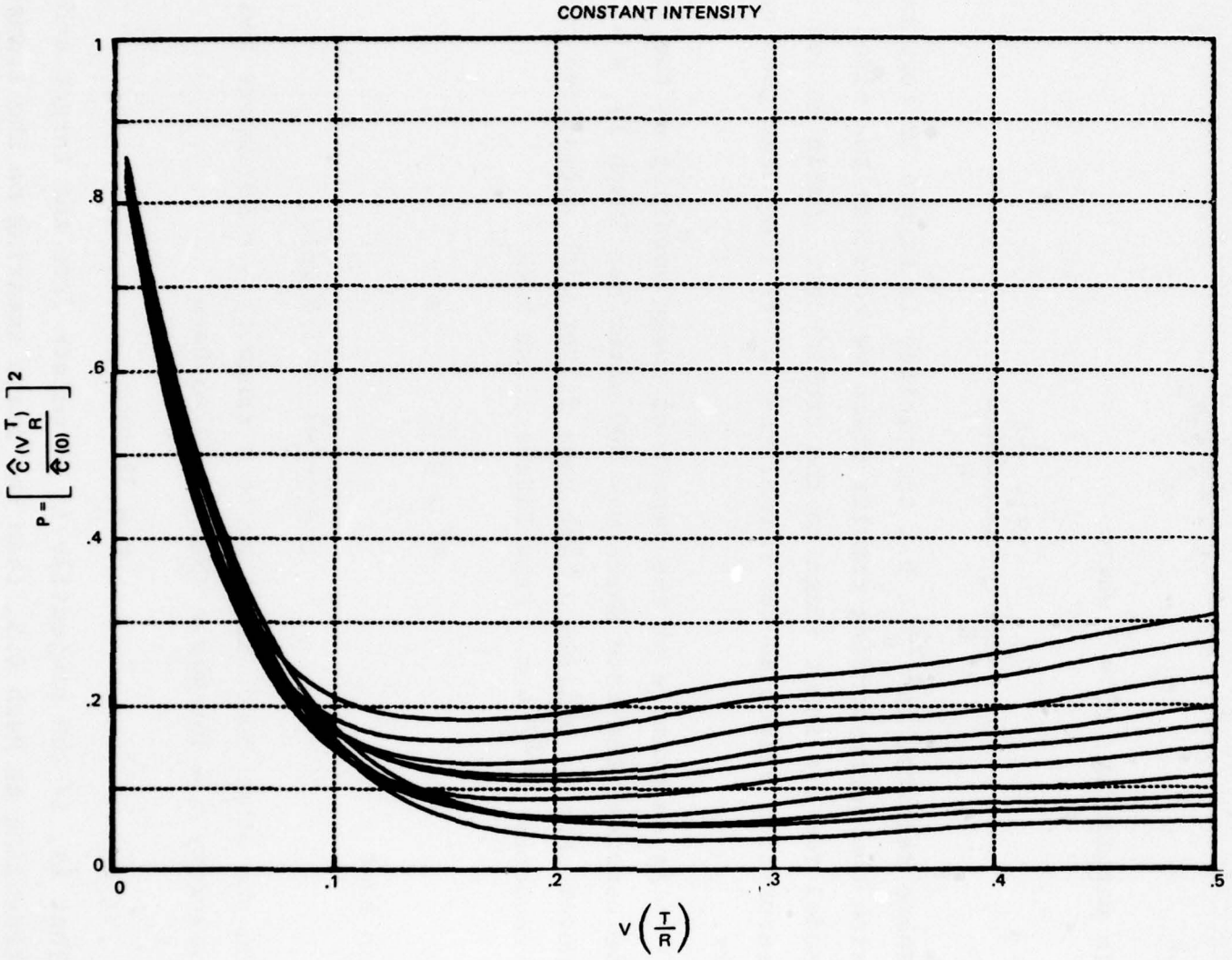

Fig. 11c Variation of Correlation Signal Due to Exposure Time (VT/R) Smearing for Constant Image Intensity and Various Cutoff Frequencies (BL/2). ($\frac{BL}{2}$ from 2.5π to 5π)

where

$$k = \frac{4}{\pi^2} \frac{A_3 \int_0^{BL_y} \frac{\sin r}{r}\, dr + A_4 \int_0^{BL_x} \frac{\sin r}{r}\, dr}{1 - \frac{16}{\pi^2} A_3 A_4} \tag{39}$$

In particular, $P_I = \frac{1}{2}$ where

$$\frac{vt}{R} = \frac{2(1 - \frac{1}{v^2})}{k}$$

These results, for $\left|\frac{vt}{R}\right| < 0.1$ are plotted in Figure 12 together with the corresponding results where we consider the fixed flux model for the input image to the transducer. Again we see the saturation effect as the normalized cutoff frequency goes beyond 2π.

As an example of the impact of image smearing as the system we consider the case where v = 300 meter/sec (Mach 1), R = 10 meter, and we utilize a high pass filter with normalized cutoff frequency of $\frac{BL}{2} = \pi$. From Figure 12 we have

$$\frac{vt}{R} = 0.1$$

so that

$$t = \frac{0.1\ R}{v} = 3.3 \text{ msec.}$$

On the other hand, if we go to a range of R = 50 meters and a velocity v = 150 m/sec (Mach 0.5) we have

$$t = 32 \text{ msec.}$$

That is, if the projectile is 50 meters from the target and traveling at Mach 0.5, then the image smearing on the transducer will reduce the correlation plane signal power by a factor of 1/2

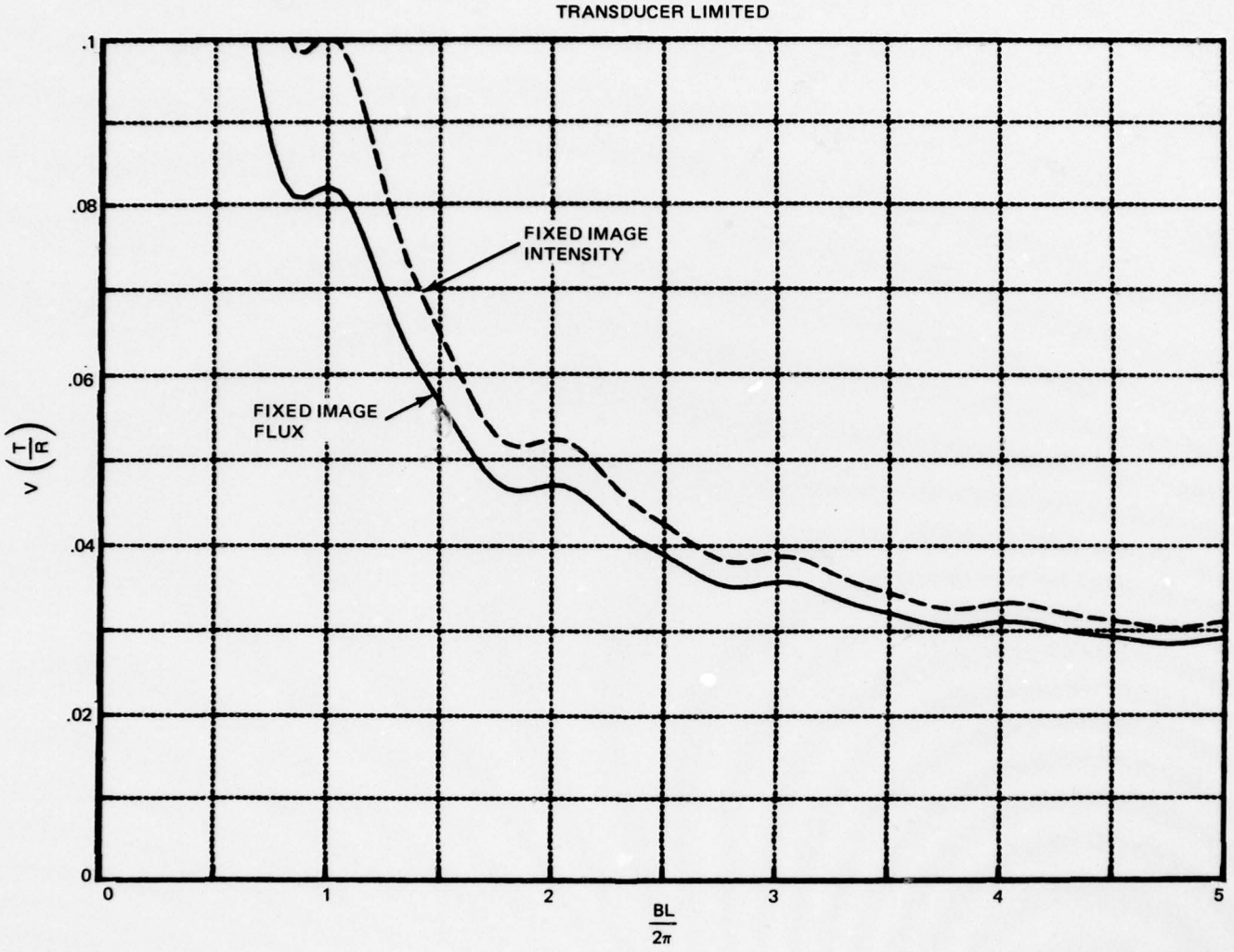

Fig. 12 Transducer Exposure Time (VT/R) Before Peak Correlation Signal Drops by 1/2 Due to Image Smear for Various High Pass Filter Cutoff Frequencies (BL/2π)

compared to the signal if the image had not been smeared; this implies the need to have a transducer response time less than 32 msec. to avoid this penalty.

9. OMFIC IMPACT UPON A REPRESENTATIVE SYSTEM DESIGN

Based upon the preceding analyses one might consider the "system" aspects of the OMFIC configuration. Specifically, what performance could we expect in a guided projectile (GP) system?

The OMFIC "guidance system" will provide a specific target identification (i.e., differentiation of an M-60 from a T-62) and require a relatively modest memory bank in order to provide guidance information to the GP. In particular, for subsonic velocities the memory bank positional requirements will be about 360.

With this memory bank and the current technology transducer, the GP has the capability of providing continued guidance for the GP from an initial acquisition range of 1.5 km to within approximately 50 meters from the intended target, and provide a maximum range uncertainty of ±5 meters to the aerodynamic guidance system for the last update.

In order to maintain a correlation signal equal or greater than -3dB fromthe peak auto-correlation value, the transducer must "record" an image in about 30 msec or less (at $M_f \sim 0.5$). This is somewhat equivalent to having the transducer operate at a standard television frame rate, a not impossible task based upon current technology. This result is based upon an uncompensated scale change effect upon the correlation signal and agrees with the situation where update (transducer) is dictated by having a sequence of continuous range "bins." However, if the detector response time dictates guidance rates, it will be about one-third faster and thus, press current transducer technology.

Thus, within the foregoing limitations the OMFIC system is capable of providing a GP with target identification and projectile guidance. In some projectile (or missile) cases it is understood that the aerodynamic response time is longer so that the OMFIC approach becomes more viable.

10. REFERENCES

1. Royce, G., "Gun Launched Guided Projectiles (U)," Vol. III, Fifth Conference on Laser Technology, Monterey, California, April 1972 (Confidential).

2. Ohlhoff, E., Vicars-Harris, M., and Bashe, R., "Artillery Launched Television," SPIE/SPSE Conference East, Reston, Virginia, March 1976.

3. System Specification for Projectile, 155 mm Cannon Launched Guided, XM712 (U); Specification No. WC-A-007-001-X, 25 June 1976. (Confidential).

4. Grumet, A. et al., "Optical Matched Filter Image Correlator," Grumman Research Department RE-512, Final Report on Contract DAAK-02-74-C-0275, May 1975.

5. Reich, A., "Optical Matched Filtering for Missile Guidance," Final Report on Contract N00019-74-C-0186, April 1975.

6. Leib, K. G., Bondurant, R. A., and Hsiao, S., "Optical Matched Filtering Techniques for Automatic Interrogation of Aerial Reconnaissance Film," Grumman Research Department Report RE-524, Final Report on Contract DAAG53-75-C-0199, September 1976.

7. Van der Lugt, A. B., "Signal Detection by Complex Spatial Filtering," IEEE Trans. Int. Theory, Vol. 10, No. 2, 1964.

8. See Reference to Table 5.2 in H.E. Brown, Et al, "Analysis of Optical Imaging Systems Using Modulation Transfer Functions," University of Texas, Defense Research Laboratory, March 1968.

9. Leib, K.G., Wohlers, M.R. and Herold, R., "Baseline Test of a Matched Filter Correlator for Screening Aerial Reconnaissance Film," Electronic Industries Association Conference on Automatic Image Pattern Recognition, Silver Springs, MD., May 1977.

10. Gara, A. D., "Real Time Optical Correlation of 3-D Scenes," Appl. Opt., Vol. 16, pp. 149-153, January 1977.

11. Proceedings of the SPIE Conference on Optical Information Processing, Vol. 83, San Diego, California, August 1976.

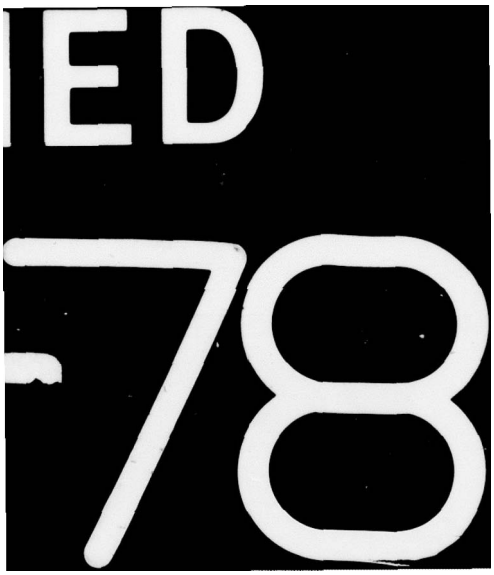
ED
78